Modelling short-term variability in carbon and water exchange in a temperate Scots pine forest

M. H. Vermeulen[1*], B.J. Kruijt[1,2], T. Hickler[3,4,5], P. Kabat[1,6]

[1] Wageningen University, Department of Earth System Science, Wageningen, The Netherlands

[2] Alterra, WageningenUR, Climate Change and Adaptive Land and Water Management, Wageningen, The Netherlands

[3] Biodiversity and Climate Research Centre (BiK-F), Senckenberganlage 25, 60325 Frankfurt am Main, Germany

[4] Goethe University, Department of Physical Geography, Altenhöferallee 1, 60438 Frankfurt am Main, Germany

[5] Senckenberg Gesellschaft für Naturforschung, Senckenberganlage 25, 60325 Frankfurt am Main, Germany

[6] International Institute for Applied Systems Analysis, Laxenburg, Austria

[*] Corresponding author. Postal address: Wageningen University, Dpt. of Earth System Science, PO Box 47, 6700 AA Wageningen, The Netherlands. Tel: +31 317 485773. E-mail address: Marleen.Vermeulen@wur.nl.

Abstract

Vegetation – atmosphere carbon and water exchange at one particular site can strongly vary from year to year, and understanding this interannual variability in carbon and water exchange (IAV_{cw}) is a critical factor in projecting future ecosystem changes. However, the mechanisms driving this IAV_{cw} are not well understood. We used data on carbon and water fluxes from a multi-year Eddy Covariance study (1997–2009) in a Dutch Scots pine forest and forced a process-based ecosystem model (LPJ-GUESS) with local data to, firstly, test whether the model can explain IAV_{cw} and seasonal carbon and water exchange from direct environmental factors only. Initial model runs showed low correlations with estimated annual gross primary productivity (GPP) and annual actual evapotranspiration (AET), while monthly and daily fluxes showed high correlations. The model underestimated GPP and AET during winter and drought events. Secondly, we adapted the temperature inhibition function of photosynthesis to account for the observation that at this particular site, trees continue to assimilate at very low atmospheric temperatures (up to daily averages of −10 °C), resulting in a net carbon sink in winter. While we were able to improve daily and monthly simulations during winter by lowering the modelled minimum temperature threshold for photosynthesis, this did not increase explained IAV_{cw} at the site. Thirdly, we implemented three alternative hypotheses concerning water uptake by plants in order to test which one best corresponds with the data. In particular, we analyse the effects during the 2003 heatwave. These simulations revealed a strong sensitivity of the modelled fluxes during dry and warm conditions, but no single formulation was consistently superior in reproducing the data for all time scales and the overall model-data match for IAV_{cw} could not be improved. Most probably access to deep soil water leads to higher AET and GPP simulated during the heat wave of 2003. We conclude that photosynthesis at lower temperatures than assumed in most models can be important for winter carbon and water fluxes in pine forests. Furthermore, details of the model representations of water uptake, which are often overlooked, need further attention, and deep water access should be treated explicitly.

Keywords: interannual variability, Eddy Covariance, photosynthesis, evapotranspiration, dynamic vegetation model, *Pinus sylvestris*.

1 Introduction

Carbon and water fluxes at one particular site can strongly vary from year-to-year (e.g. Goulden et al., 1996; Yamamoto et al., 1999; Baldocchi et al., 2001). This interannual variability in net ecosystem exchange (NEE) and actual evapotranspiration (AET) is observed across different geographical regions and ecosystem types, and understanding interannual variability in carbon and water fluxes (IAV_{cw}) is crucial for projections of future ecosystem changes and feedbacks on climate. However, little is known about the processes determining this year-to-year variation. Numerous studies have tried to relate IAV_{cw} to climatic variables and local ecosystem responses to droughts, fires or deforestation (e.g. Goulden et al., 1996; Yamamoto et al., 1999; Aubinet et al., 2002; Hui et al., 2003; Williams et al., 2008; Sierra et al., 2009; Weber et al., 2009; Yuan et al., 2009), but no clear picture has yet emerged.

Process-based biogeochemical and vegetation models capture the response of terrestrial ecosystems to mean climatic drivers reasonably well at diurnal and seasonal time scales, but not at yearly and longer time scales (Keenan et al., 2012). At the global scale, some vegetation models reproduce interannual variability in terrestrial net primary production and atmospheric CO_2 growth rates well (Peylin et al., 2005; Ahlström et al., 2012; Sitch et al., 2013), but large uncertainty exists at smaller spatial scales. Only few studies have quantified the extent to which these models can reproduce observed IAV_{cw} at the regional and site scale (Peylin et al., 2005; Keenan et al., 2012). Despite the uncertainties, such models are widely used to project future changes in vegetation and ecosystem functioning. Some of these model simulations suggest the potential for severe vegetation changes across major global biomes in the future: for example Amazon forest die-back/greening, as well as substantial shifts in potential natural vegetation distributions for boreal and Mediterranean forests (e.g. Lenton et al., 2008; Rammig et al., 2010; Hickler et al., 2012), and alternative vegetation states under elevated atmospheric CO_2 (e.g. Higgins and Scheiter, 2012). Such vegetation changes would also feed back on regional and global climate (e.g. Cox et al., 2000; Naeem, 2002; Sitch et al., 2003; van den Hurk et al., 2003; Arora and Boer, 2005; Bonan, 2008; Pitman et al., 2009; Wramneby et al., 2010), and can affect the long-term terrestrial carbon balance profoundly. Therefore it is crucial that these models accurately reproduce IAV_{cw} across all spatial scales.

To provide insight in the climate change impacts on the terrestrial carbon balance in the long term, both short- and long-term vegetation responses to a constantly changing environment should be better understood and represented. This implies better model representations of indirect short-term processes such as the mechanisms governing vegetation phenology (Cleland et al., 2007; Kramer and Hänninen, 2009; Wolkovich et al., 2012), dynamic carbon and nutrient allocation (Litton et al., 2007; Epron et al., 2012; Franklin et al., 2012), photosynthetic temperature acclimation (Gea-Izquierdo et al., 2010), as well as better representations of indirect long-term processes such as soil, nutrient and carbon dynamics. Before addressing these complex process representations within models, however, it can be useful to test whether IAV_{cw} can be explained by rather simple relationships with direct environmental drivers, such as drought, temperature and radiation, which can affect, e.g., photosynthesis and soil respiration rather directly and instantaneously. Factorial experiments with a dynamic vegetation model can then be used to generate hypotheses concerning simple and/or complex interactions of processes driving IAV_{cw}. These vegetation models can be expected to capture at least some of the complexity of real ecosystems, and the factorial experiments can be used, for example, to keep certain environmental drivers constant (i.e. switching of their effect, e.g. Hickler et al., 2005), or to implement different hypotheses concerning the most important processes within an ecosystem. The latter can also be achieved by data-model intercomparisons with several models, that differ in their process representation (e.g. Medlyn et al., 2015). In this study, the factorial model experiments refer to model setups with different process representations. With this purpose in mind, we used a long time series of Eddy Covariance measurements at a well-researched forest site (Loobos, a Scots pine forest on sandy soils in the Netherlands) and a DGVM (LPJ-GUESS; Smith et al., 2001) parameterized for the site. The observed interannual variability in NEE at Loobos is comparable to that found at sites with similar vegetation composition and climate (Carrara et al., 2003), but this interannual variability cannot be explained directly from climate variables (Jacobs et al., 2009; Kruijt et al., 2009). Previous analyses suggest that temperature is an important driver of ecosystem respiration at this site, and the remaining variation can be related to local extremes, such as drought, storm damage, and snowfall in winter (Moors et al., 2014). Luyssaert et al. (2007) thoroughly analysed observational Loobos data and proposed that photosynthesis variability is the main driver of interannual variability in NEE, suggesting that short-term ecophysiological responses play an important role.

In this study, we first tested whether LPJ-GUESS can reproduce the observed IAV_{cw} and seasonal carbon and water exchange at the Loobos site from direct environmental factors only. LPJ-GUESS combines detailed vegetation demographics and dynamics, with mechanistic representations of short-term plant physiological processes. This combination makes the model a good platform to study IAV_{cw}, because we can simultaneously study the effects of environmental and ecosystem drivers on modelled IAV_{cw}. Secondly, we tested whether using alternative model formulations and parameters can explain model error for this single site. We performed these secondary tests, because in the first test we observed systematic biases during winter periods and drought events. Therefore, we analysed the photosynthesis response to temperature during winter periods, and we analysed the response to drought events by comparing alternative plant water uptake parameterizations.

2 Methods

2.1 Study site and observation datasets

2.1.1 Study site

Loobos (coord: 52°10'04” N, 05°44'38” E) is a planted Scots pine forest that is approximately 100 years old and located in bare sandy soil at the Veluwe forest in central Netherlands. The dominant tree species is *Pinus sylvestris* and understory vegetation consists mostly of the grass *Deschampsia flexuosa* and mosses. *Vaccinium myrtillus* and various species of lichen make up the remaining understory vegetation, and the site “suffers” from encroachment of *Prunus serotina*. The landscape consists of vegetated sand dunes that create a bumpy topography with elevations varying several meters and the local groundwater levels are strongly influenced by this local topography (Moors, 2012). The average tree height is approximately 17 m, and tree density is 478 ha^{-1}. For more information on the site, and a complete overview of its measurement instrumentation and description, see http://climatexchange.nl/sites/loobos/, Dolman et al. (2002), Schelhaas et al. (2004) and Elbers et al. (2011).

2.1.2 Eddy covariance data

Eddy covariance (EC) and meteorological measurements have been continuously collected at this site since 1995 and these data are part of the FLUXNET database (Baldocchi et al., 2001). EC instrumentation is positioned on a mast extending 3 m above a 23 m scaffolding tower. In addition to EC and meteorological measurements, CO_2-concentrations are measured at five levels in the canopy: 24.4, 7.5, 5.0, 2.5 and 0.4 m above ground. The tower footprint stretches to several hundred meters, while the forest extends for more than 1.5 km in all directions from this point. EC data are processed to half-hourly corrected fluxes with the instrumentation and method described in Elbers et al. (2011). These data are quality checked, flagged and, if necessary, gap filled and split up in gross primary productivity (GPP) and ecosystem respiration (R_{eco}), using the online EC gap-filling and flux partitioning tool at http://www.bgc-jena.mpg.de/~MDIwork/eddyproc/ (7 April 2014). We used this gap-filled dataset to calculate all EC and meteorological variables on a daily time step. Flux partitioning of measured Net Ecosystem Exchange (NEE) to estimate GPP follows Reichstein et al. (2005), i.e., GPP = R_{eco} – NEE. Since our dataset follows the standard FLUXNET database format, R_{eco} and GPP are both positive quantities whereas negative NEE represents a net carbon uptake by the vegetation. As a result, GPP estimates can have a negative sign in this dataset and represent a net carbon loss of the vegetation. By definition, negative GPP cannot occur in a biological sense, but negative GPP values were not omitted from the dataset to preserve original scatter.

2.1.3 Additional site data

Sap flow measurements on *Pinus sylvestris* are available for 1997 and 1998 using tissue heat balance systems (details in Moors et al., 2012), and for 2009 using Granier thermal dissipation probes. Soil moisture data are available for all years considered within this study (1997–2009), and measured with frequency domain sensors at 5 different depths: 0.03, 0.10, 0.25, 0.75 and 2.0 m. In 2005 all sensors were replaced and positioned at different depths: 0.00 (aboveground litter), 0.03, 0.20, 0.50 and 1.0 m. For comparison with model data, available soil moisture (excluding the litter sensor) was averaged for an upper soil layer (0–50 cm), and a lower layer (50–150 cm). Additional site measurements at less frequent intervals include the leaf area index (LAI) of trees and, to a lesser extent, the understory.

2.2 Model description

LPJ-GUESS (Smith et al., 2001) is a flexible, modular modelling platform to simulate vegetation dynamics and biogeochemical cycles from local to global scales. It combines mechanistic representations of physiological and biogeochemical processes from LPJ-DGVM (Sitch et al., 2003), with the more detailed descriptions of vegetation dynamics and vegetation structure of forest gap models (FORSKA, Leemans and Prentice, 1989). The model version used in this study includes an improved hydrological scheme (Gerten et al., 2004) and an adaption for European vegetation which is mainly based on dominant tree species rather than plant functional types (PFTs) (Hickler et al., 2012). Vegetation growth is simulated on patches of 1000 m^2, where neighbouring tree individuals compete for space, light and water. On a patch, each tree individual is simulated, but individuals of the same age class (cohort) are identical. Several replicate patches (here 100) are calculated to characterise vegetation over a larger area and account for stochastic processes (establishment, mortality and disturbance events). The model is driven by daily values of temperature, precipitation and radiation, and information on atmospheric CO_2-concentrations and soil texture. The daily calculations of carbon and water fluxes between vegetation and atmosphere are mechanistically simulated in one ‘canopy exchange’ module.

2.2.1 Photosynthesis calculation

Photosynthesis – with distinction between C_3 and C_4 plants – is based on the original scheme proposed by Farquhar, as simplified by Collatz et al. (1991, 1992), and adapted from the BIOME3 model (Haxeltine and Prentice, 1996a, b). Daily gross and net leaf-level daytime photosynthesis are calculated as a function of atmospheric CO_2 concentrations, air temperature, photosynthetically active radiation (PAR), day length, and canopy conductance. APAR, the fraction of absorbed PAR captured by the vegetation, is calculated from the leaf area index with Beer's law. Leaf respiration linearly scales with Rubisco enzyme capacity. In the absence of water stress, photosynthesis is limited by two main processes that co-vary: the response of photosynthesis to APAR (J_e), and the limitation of photosynthesis by Rubisco enzyme activity and CO_2 (J_c). The rate of carbon assimilation linearly scales with APAR until maximum Rubisco activity is reached. Maximum Rubisco activity is calculated daily under the assumption that sufficient leaf nitrogen is available at the point that the marginal cost by respiration of enhanced carbon gain is zero. This leads to Rubisco activity itself also being proportional to daily APAR (the optimality hypothesis, Haxeltine and Prentice, 1996a). Two environmental stressors that can directly affect modelled daily photosynthesis are temperature and water availability. These are discussed in more detail below.

2.2.2 Temperature dependence of photosynthesis

The parameters governing maximum carboxylation capacity (V_m), as well as parameters describing saturation of Rubisco, oxygen consumption and photorespiration, follow enzyme kinetics and are thus temperature dependent. In addition, when water is not limiting, photosynthesis is made temperature dependent through a temperature scalar function (Fig. 1, see Sitch et al., 2008; function *ftemp* in Sitch et al., 2003):

$$t_{scalar} = \frac{1 - 0.01e^{4.6/(pstemp_{\max} - pstemp_{high})(T_c - pstemp_{high})}}{1 + e^{(k_1 - T_c)/(k_1 - pstemp_{\min})*4.6}} \quad (1)$$

with

$$k_1 = (pstemp_{\min} + pstemp_{low})/2 \quad (2)$$

t_{scalar} (unitless) is a temperature inhibition function that limits photosynthesis at low and high temperatures, where T_c is the daily atmospheric temperature. This scalar is used for the calculation of light-limited photosynthesis (J_e) and carboxylation-limited photosynthesis (J_c) through parameter c_1 (Eq. 11 in Haxeltine and Prentice, 1996b):

$$c_1 = \alpha * t_{scalar} * \frac{(c_i - \Gamma_*)}{(c_i + 2\Gamma_*)} \quad \text{(from Sitch et al., 2003, Eq. 17)} \tag{3}$$

where α is the effective ecosystem-level quantum efficiency, c_i the intercellular partial pressure of CO_2, and Γ^* the CO_2 compensation point (further explanation and equations in Sitch et al., 2003). t_{scalar} is defined with a PFT/species-specific lower and upper limit for photosynthesis ($pstemp_{min}$, $pstemp_{max}$) and an optimum temperature range ($pstemp_{low}$, $pstemp_{high}$) (Larcher, 1980; Table 3.7). This optimum range (i.e. the upper plateau in Fig. 1) represents an effective temperature response of many enzyme and transport related processes. Within this optimum range, t_{scalar} equals unity (i.e. t_{scalar} is equal to 1), and creates a slight rise in maximum carboxylation capacity (V_m), but reduces photosynthesis with increasing temperature. Outside this optimum range, both light-limited photosynthesis and V_m are reduced. Temperatures outside the $pstemp_{min}$, $pstemp_{max}$ range result in zero photosynthesis. So, apart from the abovementioned processes that follow enzyme kinetics, and are thus temperature dependent, t_{scalar} imposes an additional temperature stress on photosynthesis calculations.

2.2.3 Photosynthesis under water stress

Plants experience water stress when water supply (S) is smaller than the demand (D). Supply is proportional to the available soil moisture in the rooting zone (wr) and the maximum possible transpiration rate under well watered conditions (E_{max}; 5 mm day^{-1} following Haxeltine and Prentice, 1996b):

$$S = E_{\max} * wr \tag{4}$$

The demand is simulated with an empirically calibrated hyperbolic function of non-water stressed canopy conductance and the equilibrium transpiration (Huntingford and Monteith, 1998; Gerten et al., 2004). If the water supply is lower than the demand, canopy conductance is reduced until evapotranspiration (transpiration and evaporation from the canopy and the soil) equals the demand. This limits CO_2 diffusion into the leaves, expressed in a reduction of the ratio of internal to atmospheric CO_2-concentration, c_i/c_a. A lower c_i/c_a ratio leads to a reduction of photosynthesis.

2.2.4 Plant water uptake parameterizations

The soil hydrology is represented by a simple bucket model with two layers. The upper layer (l_1) is 50 cm deep, and the lowest layer (l_2) is 100 cm deep. Available soil moisture wr is the ratio between current soil water content and plant-available water capacity. The latter is dependent on soil type and texture (Sitch et al., 2003). The model offers the following three methods to calculate available soil moisture in the rooting zone (Supplement, Fig. S1): Method 1: *wr* is independent of soil water content until wilting point (*wr_rootdist*). This is the current standard used in most studies with LPJ-GUESS (T. Hickler, personal communication, 2013), Method 2: *wr* is influenced by a species specific drought tolerance value (Table 1). In response to declining soil water, drought-tolerant species reduce transpiration less than drought-sensitive species, and therefore have greater relative uptake rates (*wr_speciesspecific*; see Schurgers et al. (2009) for an application of LPJ-GUESS using this formulation), and Method 3: *wr* declines linearly as a function of soil water content (*wr_wcont*, which is used in most studies with LPJ-DGVM (description in Haxeltine and Prentice, 1996b)). A more detailed description of each method with equations is provided in the Supplement.

2.3 Modelling setups

2.3.1 Default modelling setup

As a driver, we used the site-specific meteorological dataset of daily averages from 1997 to 2009, and this dataset was repeated consecutively during the model run. To simulate the establishment of a Scots pine forest on a bare sand soil, we ran the model for 105 years (as a "spin up" period), so that the simulated forest would have a stand age and soil carbon pools comparable to our study site. Only *Pinus sylvestris* and herbacious vegetation with C_3 photosynthesis (to represent the understory) were allowed to establish. Since *Prunus serotina* encroachment is relative recent and actively suppressed, we did not include this species in the model. Furthermore, the site has not been disturbed by fire since its establishment so we also did not include fire disturbance in the model. Finally, we used the averaged results of 100 replicate patches to account for any stochastic effects on vegetation establishment. All PFT/species-specific parameters for this study were taken from Hickler et al. (2012), except for two parameters (Table 1, bold values). Maximum coldest month temperature for PFT/species establishment (T_{c,max_est}) was set to limitless for *P. sylvestris*, to ensure establishment of these planted trees at the temperate climate of Loobos. Specific leaf area (*sla*) for *P. sylvestris* was set to a site-specific value based on measurements (Table 1). For comparison of modelled carbon and water fluxes to EC data, modelled daily GPP, NEE, R_{eco}, plant transpiration, soil evaporation and canopy interception are available. Modelled AET was calculated as the sum of plant transpiration plus evaporation from the soil and canopy. Water uptake was set to the default used in previous studies with this model: *wr_rootdist*.

2.3.2 Alternative temperature response function

Based on the results of the default model run (Sect. 3.1), we decided to decrease the lower temperature limit ($pstemp_{min}$, Eqs. 1 and 2) for Scots pine to allow photosynthesis on frost days. To compare our findings with existing data, and to determine a suitable lower temperature threshold for photosynthesis of mature Scots pine forests at temperate sites, we identified a limited number of previous studies relevant to the situation at Loobos. For example, James et al. (1994) measured photosynthesis and growth of Scots pine along a latitudinal gradient in Scotland (Creag Fhiaclach, Cairngorms National Park), and found that valley trees displayed higher photosynthesis rates in winter compared to those growing at higher latitudes. Teskey et al. (1994) report net photosynthesis in winter when there are no severe frosts and the soil is not frozen. Linder and Troeng (1980) report minimum atmospheric temperatures of −7 °C for net photosynthesis for *P. sylvestris* in southern Sweden, which is slightly higher than, but in a similar range as, observed at our study site Loobos. Sevanto et al. (2006) show net uptake of carbon for many freezing days during the winter of 2002/03, and positive uptake in all previous 7 years except during January in southern Finland. At Brasschaat, a slightly younger (compared to Loobos) temperate mixed-deciduous-coniferous forest in Belgium, net carbon uptake was observed only in the winter of 2001 (Carrara et al., 2003). At this site, however, not all trees are evergreen so winter LAI is lower compared to our study site.

In addition to the literature review, we analysed several types of available observation data in three different ways to determine a suitable lower temperature threshold. Analysis 1: we selected days from the EC dataset between late November and late February, with average daily temperatures below 0 °C (n = 226). In order to see the effect of temperature on observed GPP and AET, days with low radiation were excluded: total net shortwave radiation received > 2 MJ day^{-1}, which is an average of about 75 W m^{-2} for a winter day with 6 h of daylight. For days that met these criteria (n = 175), modelled and observed data were binned to temperature classes of 2° ranging from <= −10 to 0 °C; Analysis 2: from a different study (Abreu, 2012), we included a fitted temperature response curve for maximum GPP (indicated as GPP_{1000}). Abreu calculated GPP_{1000} following Jacobs et al. (2007), using half-hourly EC data between 1997 and 2011. Due to the large number of data points needed to calculate

GPP_{1000}, these results are only available for 5° temperature bins between −5 °C and 35 °C; Analysis 3: a two-day measurement campaign with a portable ADC- LCpro (ADC BioScientific, Hoddesdon, UK) was carried out at the study site in 2012 to measure leaf photosynthesis on days with temperatures below 0 °C (description and results in Supplement).

Based on the outcome of the literature review and observation data analysis, this model experiment uses a lower threshold for *P. sylvestris* photosynthesis ($pstemp_{min}$) of −10 °C. Other than this lower threshold, this model setup does not differ from the default model setup.

2.3.3 Alternative plant water uptake parameterizations

In this setup, PFT/species-specific parameter values remained unchanged compared to the default setup, but we ran the model for all three available water uptake parameterizations (Sect. 2.2.3): (1) the default run (S1), using the standard '*wr_rootdist*' uptake, (2) a species specific water uptake run (S2), and (3) a linear uptake run (S3). Figure S1 shows the different water uptake response curves for *P. sylvestris* and C_3 grasses. Response curves differ between species as a result of PFT/species-specific root distributions ($root_{distr}$, Table 1): C_3 grass has 90% of its roots prescribed in the upper soil layer (0–50 cm), and 10% in the lowest layer (50–150 cm), for *P. sylvestris* this is 60 and 40%, respectively. In the case of species specific water uptake, the response curves also differ because grass and *P. sylvestris* have different assumed drought tolerance ($drought_{tol}$, Table 1). Species specific water uptake is represented with response curves S2a and b, with C_3 grass having larger relative uptake rates than *P. sylvestris* under declining soil water content. Linear decline of supply with decreasing soil water results in similar uptake rates for both *P. sylvestris* and C_3 grasses, since modelled water uptake is independent of root distribution in this parameterization (Supplement, Fig. S1, response curve S3).

As a control, we include one additional model run (S4) using the standard water uptake method (*wr_rootdist*), but eliminated plant water stress by fixing *wr* to 1.0 so that supply is always equal to E_{max} (Eq. 4). Model results of setups S1–S4 were investigated in more detail for the summer period to determine the effect of a heat wave and corresponding drought on the observed and modelled carbon and water fluxes.

2.4 Statistical tests

To test how well the model is predicting the observed values of GPP and AET, we applied a linear regression through the origin as well as Pearson correlation tests. If the slope of the linear regression were equal to unity, our model would match the observed data with no systematic bias. Statistically significant differences from 1.0 in the regression slope were determined by a two-sided *t* test at a threshold of $P = 0.05$. The root mean squared error (RMSE) between model and data was calculated as a measure of prediction accuracy, i.e., "goodness-of-fit". Additionally, a two-sided paired Wilcoxon ranking test was performed to determine if observed and modelled samples follow similar distributions. Only when *P* values of this test are larger than 0.05, we accept that the model produces a data distribution that is similar to the data distribution of the observations.

3 Results

3.1 Default modelling setup

The general site characteristics of Loobos are well represented by the default modelling setup (S1, Table 2): modelled LAI for Scots pine is 1.5, declining to 1.4 between 1997 and 2009. This LAI is just below the observed site average of 1.62 between 1997 and 2009 (minimum 1.44 in 2007, maximum 1.78 in 2009). Modelled LAI for C_3 grasses is higher than observed (2.4 and 1.0 respectively), but few measurements of understory grass LAI were available for validation and none for mosses. Modelled aboveground biomass estimates are close to available observations.

Figure 2 shows the interannual and monthly variability in GPP and AET. Table 3 summarizes the goodness-of-fit-values for GPP and AET. The model shows good correlations on daily and monthly time scales (Fig. 2c and d). Monthly correlations are significant (0.92 for GPP, and 0.87 for AET), indicating that the model is accurately capturing the seasonal pattern of both fluxes. This is also visible in Fig. 3a and b. In contrast, we find poor correlations on the annual time scale: annual totals for GPP and AET are of the same order of magnitude as observed values, but the observed IAV_{cw} is not captured well by the model for water nor for carbon (Fig. 2a and b). The modelled data distribution is similar to observations (Table 3, bold values), but correlation coefficients are low and not significant (0.22 and 0.20 for GPP and AET, respectively).

The monthly scatterplots (Fig. 2c and d) display systematic model biases during certain periods. Fluxes are underestimated in winter, overestimated in spring/early summer and slightly underestimated in fall (Fig. 2c and d). In summer (mainly in August and July), large deviations from the 1 : 1 line can be seen, which we could directly relate to periods with high atmospheric temperatures and low precipitation. Figure 3 shows these deviations per month in more detail.

3.2 Alternative temperature response function

3.2.1 Observed temperature response

According to the EC data, the vegetation at Loobos is able to keep assimilating carbon even at temperatures below 0 °C (Fig. 4). In the fitted response curve of half-hourly EC fluxes, maximum GPP for the lowest temperature class (−5 to 0 °C, Fig. 4a) is 1.8 μmol m^{-2} s^{-1}, which corresponds to 1.87 g C m^{-2} day^{-1}. Figure 4b shows temperature-binned daily GPP on sunny days, and the response to temperatures below −10 °C. The lower temperature limit in our observation data, i.e., where average GPP approaches 0, is found when temperatures are below −8 °C. Note that the number of data points, however, in temperature class −8 to −10 °C is relatively low (n = 2). To further check data for this particular temperature class, we included half-hourly EC data for two such days (Supplement, Figs. S4 and S5). On these days, NEE becomes negative and strongly responds to radiation, especially around noon. The average assimilation capacity for all the example dates in Figs. S4 and S5 correspond well with the upper quartile of daily observed GPP as shown in Fig. 4b. As can be expected, average observed GPP per day is slightly lower than the maximum capacity for a certain temperature class. The leaf level measurements (Supplement, Fig. S6) also show active assimilation when atmospheric temperatures were below 0, with *P. sylvestris* needles strongly responding to radiation. A linear regression through these data points gives a minimum of −10.1 °C.

All three data sources indicate that carbon assimilation stops when temperatures fall below −10 °C (Fig. 4b), and when a prolonged period of extremely cold temperatures is observed. The latter was the case in early January 1997, even on days with high radiation and temperatures between −6 and −8 °C (Fig. 4b, 1st and 2nd quartile).

3.2.2 Modelled temperature response

Based on the outcome of the literature review and observation data analysis, this model setup used a lower threshold for *P. sylvestris* photosynthesis ($pstemp_{min}$) of −10 °C. The effect of changing the temperature response in LPJ-GUESS on the seasonal trend of GPP and AET is shown in Figs. 3, 5 and 6. Changing the lower boundary for photosynthesis for *P. sylvestris* to

−10 °C (Fig. 1) results in higher winter estimates for GPP (Figs. 3a and 5a) and, to a lesser extent, for AET (Figs. 3b and 5b). The latter can be expected, since interception and soil evaporation do not change and there is only a slight increase in plant transpiration. When selecting days with high radiation only (Fig. 5), simulations with changed temperature response follow the distribution of daily observed GPP more closely. For the entire simulation, the overall error (RMSE, Table 3) reduces for both AET and GPP, with the exception of GPP at monthly time scales. Correlations (*r*, Table 3) do not increase for GPP, and are similar for AET over the entire simulation period. However, the Wilcoxon ranking test shows that for GPP the modelled data distribution is now matching the observed data distribution at monthly time scales more closely ($P < 0.05$). In addition, when data of only the winter months are included (Fig. 6), the slope of the regression substantially improves for GPP from 0.32 to 0.58, while keeping a similar correlation coefficient (0.80 vs. 0.78). This indicates a better match between modelled and observed results. By changing the temperature response, simulation of IAV_{cw} does not improve for the carbon fluxes, and only marginally for the water fluxes (Table 3).

3.3 Alternative plant water uptake parameterizations

Figure 7 shows modelled carbon and water fluxes on a monthly time scale for the three different water uptake parameterizations (S1–S3) and the control model setup without soil moisture stress (S4). All three uptake parameterizations appear to be equally strong in simulating the seasonal trend with correlations from 0.92–0.94 for GPP and 0.86–0.88 for AET (*r*, Table 3). During summer, the linear uptake response curve (S3) underestimates both AET and GPP more often than the species specific (S2) and default uptake (S1) parameterizations. Eliminating water stress (model setup S4), results in overestimation of fluxes during summer, increased error and lower RMSE. Moreover, using this setup both AET and GPP are overestimated in spring and summer for all years (Fig. 7a), indicating that water limitation does play an important role in Loobos.

Given the model's very simple two-layer soil hydrology (Sect. 2.2.4) and the fact that our measured soil moisture data were averaged to correspond with the model's layer depths (l_1 and l_2), seasonal soil moisture patterns are captured reasonably well between the different model setups when compared to observations (Supplement, Fig. S3). Modelled soil moisture in the upper soil layer changes more rapidly than observations suggest, and modelled moisture recharge in winter increases to higher values than observed for some years. Soil moisture measurements, however, were not always available during winter and completely absent from fall 2000 until summer 2002. Because plants are taking up water more conservatively in setup S3, modelled soil moisture is higher during the growing season for all years compared to the other two setups, and the bucket never completely empties as is often the case for the other two setups. Available sap flow data for *P. sylvestris* (1997, 1998 and 2009) show good correlations with modelled transpiration (Fig. 8, r = 0.68–0.74). For setups S2 and S3, the range of modelled plant transpiration is lower than the observed plant transpiration (0−1.5 mm day^{-1} and 0−3 mm day^{-1} respectively). For setup S1, the range of modelled plant transpiration matches that of the observations for 1997 and 1998 (0−3 mm day^{-1}). This relates directly to the shape of the response curve for each setup (Supplement, Fig. S1), where S2 and S3 reduce the water supply S more strongly than S1 in response to declining soil water. Correlations for individual years are lowest for 1997, especially for setups S2 and S3, where modelled transpiration is reduced too strongly in response to declining modelled soil water between day 100 and 300 (Supplement, Fig. S3).

On the annual time scale, species specific uptake (S2) leads to the best explanation of interannual variability in GPP in terms of correlation coefficient (Table 3), while for AET there is a small decrease compared to the default setup. Using the model setup in which soil water is not a limiting factor (S4), the model also cannot accurately capture interannual variability in GPP and AET.

3.3.1 Comparing water uptake parameterizations during a dry and wet summer

The summers of 2003 and 2005 were very different, with the 2003 heat wave over Europe affecting both managed and natural vegetation systems but each ecosystem showing different responses to the extreme heat (e.g. see Granier et al., 2007; van der Werf et al., 2007; Teuling et al., 2010). The 2003 heatwave affected the Netherlands (KNMI, 2003) especially in August, which in combination with a prolonged period of low precipitation resulted in a drought. We compare the results of the extremely sunny, warm and dry August 2003 to those of August 2005, which was a regular but very wet month. Observed soil moisture at Loobos declined considerably during the 2003 heatwave, and modelled soil water runs out earlier than observations suggest (Fig. 9, for 2003), with the exception of setup S3 and, to a lesser extent, for the lower soil layer of setup S2. For 2005, modelled soil moisture is often too low when using the default setup (S1), and water content of the upper layer changes more rapidly than observations suggest.

When comparing daily carbon and water fluxes to observations (Fig. 10) during the wet period (2005), all uptake parameterizations perform well compared to observed data, with no striking differences between uptake parameterizations in simulating GPP and AET. During the 2003 heatwave and drought however, the parameterizations show different responses. During the first half of the heatwave period (indicated by the two vertical dotted black lines in Fig. 10), there is a gradual decline in observed daily GPP and AET at the site. Given the considerable drop in observed soil water during the heatwave (Fig. 9), reductions in observed GPP and AET look considerably more gradual (Fig. 10). This suggests a possible access of the vegetation to water from deeper layers, or groundwater. The no-water stress control run (S4) clearly demonstrates there is some water stress at Loobos (both observed GPP and AET are lower than the model predicts), but all parameterizations fail to simulate the correct response. The default and species specific response curves (S1 and S2), allow PFTs and species to take up relatively more water at low soil water contents compared to the linear uptake parameterization, thereby not restricting photosynthesis as long as water remains available for uptake. We can observe this effect during the heatwave period, where the linear uptake function (S3) least underestimates GPP and AET, because there is more water available for uptake due to conservative water use, and the effects on the modelled supply are less strong at lower soil water contents (Figs. S1 and S2). The real observed response of the Loobos vegetation, however, is not reproduced using either uptake parameterization. The sensitivity of GPP and AET to declining soil moisture during the growing season is visible in Fig. S2 by plotting the residuals (modelled–observed values, so that an underestimation is depicted with a negative sign) against modelled available soil moisture (Θ). In general, the linear uptake parameterization seems to underestimate both GPP and AET more at higher soil moisture values, so with regard to the observations, this response curve imposes water stress on plants at this site too strongly.

A comparison of the three different plant water uptake response curves does not lead to identification of any setup that is clearly superior for simulating IAV_{cw} to the others (Table 3). Species specific uptake (S2) results in the smallest errors (RMSE, Table 3) on monthly and daily time scale, but on annual time scale the default uptake (S1) has the smallest error.

4 Discussion

4.1 Default modelling setup

The model reproduced the daily and monthly carbon and water fluxes equally well as shown in previous studies with LPJ-GUESS (Sitch et al., 2003; Gerten et al., 2004; Morales et al., 2005; Zaehle et al., 2005; Hickler et al., 2006). Fatichi and Ivanov (2014), using a different process-based vegetation model, similarly found very high correlations on daily and low correlations on annual time scales for GPP and evapotranspiration. However, good correlations on shorter time scales can be expected, given the strong diurnal and seasonal cycles to climatic drivers (mainly radiation and temperature). While the model produces reasonable flux estimates at daily and monthly time scales, the small deviations on these time scales lead to poor estimates of IAV_{cw} and longer time scales, which Keenan et al. (2012) demonstrated for a wide range of terrestrial biosphere models.

At some sites where needle leaf evergreen vegetation is the dominant vegetation type, year-to-year variation in fluxes can be explained by climatic and environmental drivers (e.g. disturbances) only. For example, Sierra et al. (2009) applied a process-based stand vegetation model which showed that some forests are mostly affected by short term dynamics such as disturbances, and others are more influenced by climatic controls. Duursma et al. (2009) performed a model-data comparison using a calibrated empirical photosynthesis model, and found good fits for GPP on daily to seasonal time scales for several European FLUXNET sites and, similar to this study, comparably poor fits on the annual time scale. They attributed part of this mismatch to uncertainty in the EC data, variations in LAI, and reductions in GPP as a result of soil drought. Purely observational studies at temperate coniferous forests in Brasschaat (Carrara et al., 2003, 2004) and Vielsalm (Aubinet et al., 2002), showed that climatic and ecological drivers (such as changes in LAI, phenology shifts) explain the majority of interannual variability in observed carbon and water fluxes. Our results, as well as studies by Jacobs et al. (2009), Kruijt et al. (2009) and Luyssaert et al. (2007) suggest that, in addition to direct climatic and environmental factors, ecological drivers also operate at the Loobos site.

4.2 Uncertainties in the observation dataset

For this study, the mismatch between simulated and observed fluxes both at the monthly and at the annual time scale can only be partly attributed to uncertainties in the flux data. The magnitude of the error for this dataset is estimated by Elbers et al. (2011) as 8% of annual NEE, which is a quarter of the standard deviation of annual NEE, and is small compared to other flux sites (Elbers et al., 2011, data from 1997–2010). Because GPP is estimated from NEE and night-time respiration, the errors in annual NEE, especially the notorious errors in night-time NEE due to low turbulence, propagate into GPP estimates. During winter, when relatively more data is gap-filled, this uncertainty in the data can contribute to a higher deviation between the modelled and observed results in this study.

4.3 Alternative temperature response function

4.3.1 Observed temperature response at Loobos and similar sites

We presented strong evidence that *Pinus sylvestris* continues to assimilate during winter in temperate climates, and even acts as a carbon sink during frost periods rather than as a source, as most DGVMs currently suggest (Morales et al., 2005). Falge et al. (2002) even suggest, based on their analysis of FLUXNET data, that temperate and boreal conifers should be seen as two separate classes. The observations at Loobos support this suggestion, as *Pinus sylvestris* clearly continues to assimilate in winter during all years, even when daily average temperatures drop below 0 °C. These pine trees grow in a temperate climate, and therefore experience relatively milder winters compared to the same species at boreal sites. Plants are known to acclimatize to their growing conditions, so differences in the seasonal carbon gain within species reflect to a large extent the light- and temperature environment in which they exist (Teskey et al., 1994). Plants native to a colder climate exhibit higher photosynthetic rates under colder temperatures, but, at higher latitudes, *Pinus sylvestris* is also known to display winter photo-inhibition as a result of lower winter temperatures (Berry and Bjorkman, 1980). This winter inhibition of the photosynthetic capacity is thought to be a protective mechanism against damaging combinations of low atmospheric temperatures and exposure to high irradiances that can be enhanced by snow cover. If, however, winters are warm enough, photosynthesis in evergreen forest stands can continue if enough soil water is available to meet the transpirational demand (Sevanto et al., 2006 and references therein). How long it takes for the photosynthetic capacity to diminish during extended cold periods − and possibly recover when temperatures rise again (e.g. see Suni et al., 2003a, b; Kramer et al., 2008; Kramer and Hänninen, 2009) − is not known for this site and will be investigated in a winter measurement campaign of leaf photosynthesis over the next few years.

4.3.2 Modelled temperature response

The modelled changed temperature response function had a smaller effect on simulated AET than on simulated GPP (Fig. 5). Simulated AET is calculated as the sum of plant transpiration, soil evaporation and canopy evaporation. Underestimation of canopy evaporation (interception loss) in relation to precipitation intensity in winter can play a role here. In general, measured AET fluxes during winter are high for this type of forest. At Loobos, measured AET peak values during winter are mainly the result of high interception evaporation (Elbers et al., 2010). Modelled LAI was slightly lower than observed (Table 2), which results in a lower precipitation storage capacity for the vegetation than in reality. Additionally, as the model does not explicitly handle shower intensity, and prolonged periods of low precipitation intensity occur often at the site during winter, the model underestimates interception evaporation. This underestimation of canopy interception likely contributes to underestimations of AET on the longer time scales as well.

Even when Scots pine is allowed to continue assimilating at lower temperatures, the difference between modelled and observed fluxes improves, but is not completely resolved. The shape of the temperature response curve for *Pinus sylvestris* (Fig. 1), is modelled as a steep increase from the minimum temperature ($pstemp_{min}$) to the optimum temperature ($pstemp_{low}$), which, to our knowledge, is not supported by literature but purely empirical. For this study, we identified a lack of data and literature to verify the exact shape of this response curve and instead calculated the minimum temperature threshold from the available data. Smith and Dukes (2013) reviewed the latest available methods to incorporate photosynthesis temperature acclimation into global scale models, and suggest that instead of just looking at temperature optima, shifts in the slope/intercept of the initial instantaneous temperature response could be of equal or greater importance, especially at suboptimal temperatures, and that a combination of data collection and modelling studies, such as ours, is needed to improve our understanding and realistically simulate long term responses of vegetation to temperature shifts.

The small impact of changing the temperature response function on simulating IAV_{cw} is of course related to the fact that wintertime fluxes make up only a small part of the total annual flux (average observed annual GPP for this dataset is 1284 g C m^{-2}), usually less than 10%. In contrast, the largest observed interannual difference in GPP for this period is almost twice as large at 200 g C m^{-2}. Therefore, small improvements in the winter estimates will not translate directly into good estimates and high correlation coefficients on the annual time scale.

4.4 Alternative plant water uptake parameterizations

The use of three different soil water uptake parameterizations revealed that the model can satisfactorily simulate GPP and AET during wet summers such as that of 2005. The model performed well for those years that plant transpiration for Scots pine could be compared with sap flow observations (Fig. 8). However, none of the uptake parameterizations capture the observed response in terms of GPP and AET to a drought such as occurred in the summer of 2003 (Fig. 10). In addition, none of the three parameterization consistently improved all results, nor improve simulated IAV_{cw} at Loobos.

Previous studies have demonstrated that LPJ-GUESS is sensitive to limitations in soil moisture, firstly because the parameters controlling stomatal conductance are very sensitive to plant water stress (Zaehle et al., 2005) and secondly, because the model does not account for plant ability to access water from deeper soil layers and aquifers in water-limiting situations (Hickler et al., 2006; Wramneby et al., 2008). The debate on how to improve modelling efforts in a mechanistic way, however, is still on-going. For example, Hickler et al. (2006) included plant hydraulic architecture in the global model version of LPJ, thereby changing the calculation of plant water supply to a more mechanistic scheme. This improved global simulations of AET, but the updated model requires additional PFT/species-specific parameters that are often not available and the model still underestimates summer AET at one Mediterranean test site. Verbeeck et al. (2011) tried increasing soil depth and used locally varying root profiles to improve simulations of dry-season GPP for the tropics. Such an approach, however, does not lead to the desired mechanistic model improvements because it eliminates simulated water stress completely. Furthermore, high- quality data on effective rooting depth, soil volume and deep soil water are rarely available, and deriving model parameters representing deep tap roots, sometimes growing through rock fissures or compacted soil layers, is difficult. These challenges are probably the reason why access to deep water is, to our knowledge, not captured in any DGVM. Nevertheless, we think that further efforts should be devoted to improving the current state of the art in this respect, because access to deep water is probably crucial in many ecosystems around the world.

The 2003 summer drought simulations at Loobos confirm the strong model sensitivity to drought: under dry soil moisture conditions the vegetation shows a much more gradual response in flux reduction compared to the model runs (Fig. 10). Observed soil moisture values are low and gradually decline during the heatwave (Fig. 9), suggesting the vegetation can access water from deeper layers, or groundwater. *Pinus sylvestris* is known for its ability to create long tap roots, especially when growing on sandy soils, so that water uptake is also possible from sparsely rooted deep soil layers when water becomes limiting (Jarvis, 2011).

The shape of the water uptake response curves in the model clearly has an effect on the water uptake (Supplement, Fig. S1). The exact shape of this curve, however, is both species and site specific, and remains poorly defined for global model studies that use broad PFT classifications. For *P. sylvestris*, Lagergren and Lindroth (2002) summarized uptake curves from several studies, and the reported shapes are very similar to the ones used in this study, most closely resembling *wr_rootdist* and *wr_speciespecific*. Reality probably lies in between the original linear formulation and *wr_rootdist*, because plants do not reduce transpiration immediately when soil water content declines: transpiration remains unaffected until the soil water potential reaches values at which the xylem can be damaged by cavitation. Next, depending on the strategy of the tree, transpiration is either reduced due to cavitation or to stomata closing to prevent cavitation (McDowell et al., 2008). During droughts, plants may reallocate carbon to roots instead of leaves or needles, thereby reducing their assimilation potential through reduced leaf area. Such seasonal changes in carbon allocation and phenology under drought are currently not explicitly handled in LPJ-GUESS because allocation occurs annually in the model (on the annual time scale, however, the leaf to fine root ratio adjusts to water availability). Model inaccuracies in reproducing this type of vegetation phenology and hence the simulation of seasonal cycle of CO_2 and water can lead to poorly simulated fluxes compared to observed ones. Future modelling efforts should focus on root dynamics, include the effects of groundwater uptake and shifts in carbon allocation under water stress.

5 Conclusions

Variability in ecosystem carbon and water exchange is a key aspect of ecosystem functioning, but, in many cases, the drivers are poorly understood. Here, we showed that a DGVM, when adapted to the local conditions, can reproduce daily to seasonal variability in carbon and water exchange with high correlation coefficients. Similar to other studies, however, the model cannot reproduce interannual variability. We tried to identify the driving mechanisms of IAV_{cw} by looking at systematic biases in the model output. By comparing the model to a long term dataset, we found that carbon assimilation during winter months at daily average temperatures below 0 °C is important for winter fluxes and not captured in the current parameterization of the model, which might also apply to other, similar, models. Lowering the minimum temperature threshold for photosynthesis improved the simulation of winter GPP substantially, but did not greatly improve simulations of IAV_{cw}. In addition, we demonstrated that the modelled response to drought is too strong for this site, and that none of the water uptake formulations was consistently superior in reproducing the observed response of GPP and AET. AET and GPP during the 2003 heat wave were substantially underestimated by the model, even when assuming that plants have maximum water supply until the wilting point is reached. This result and the soil water curves suggest that at this site, access to deep water is crucial for the vegetation response to extreme drought. However, our understanding of IAV_{cw} at the Loobos site still remains incomplete, as we were not able to disentangle the main drivers of IAV_{cw} at the site. As future steps we suggest that, firstly, the representations of water uptake and root growth of plants need further attention in terms of model testing and parameterization. This includes the implementation of a groundwater table and rooting access to it, and accounting for precipitation duration and intensity to make interception evaporation in winter more realistic. Secondly, estimating the amount of water stored deeper in the soil than the soil depth of common DGVMs, may be crucial for simulating the drought response of vegetation even in areas such as the Loobos site, where this was not expected. Thirdly, we want to further explore the hypothesis that IAV_{cw} is driven by short-term resource allocation of the vegetation. If past and current productivity (GPP) drive future productivity, for example via LAI changes, and these are influenced by environmental drivers and stressors such as temperature and droughts, modelling allocation and growth on a daily or monthly time step could be crucial. Because the process interactions underlying variability in ecosystem functioning are so complex that analyses with single factors, such as temperature or precipitation, often do not shed light on the mechanisms, we think that improvement of the process-based modelling and confronting these results with observations is an important complementary approach. Accurate reproduction of site-level fluxes with such models on the seasonal to annual time scale is essential for our understanding of vegetation-climate interactions and for reducing uncertainties in future projections.

Acknowledgements

This work is part of the research programme Sustainable Earth, financed by the Netherlands Organisation for Scientific Research (NWO). TH acknowledges support from the research funding programme “LOEWE-Landesoffensive zur Entwicklung Wissenschaftlich-ökonomischer Exzellenz” of Hesse’s Ministry of Higher Education. The authors are grateful to J. Elbers, W. Jans and K. Fleischer for providing Loobos field data, to M. Forrest for model support, and to P. Rocha e Abreu and L. Mossink for assisting with photosynthesis measurements and raw data analysis. We thank I. Supit for fruitful discussions and valuable comments on this manuscript.

References

Abreu, P. M.: Loobos Scots Pine Forest Data Analysis 1997−2011, Dpt. Earth System Science & Climate Change, Wageningen University, Wageningen, internal report, 2012.

Ahlström, A., Miller, P. A., and Smith, B.: Too early to infer a global NPP decline since 2000, Geophys. Res. Lett., 39, L15403, doi:10.1029/2012gl052336, 2012.

Arora, V. K. and Boer, G. J.: A parameterization of leaf phenology for the terrestrial ecosystem component of climate models, Glob. Change Biol., 11, 39−59, doi:10.1111/j.1365-2486.2004.00890.x, 2005.

Aubinet, M., Heinesch, B., and Longdoz, B.: Estimation of the carbon sequestration by a heterogeneous forest: night flux corrections, heterogeneity of the site and inter-annual variability, Glob. Change Biol., 8, 1053−1071, doi:10.1046/j.1365-2486.2002.00529.x, 2002.

Baldocchi, D., Falge, E., Gu, L., Olson, R., Hollinger, D., Running, S., Anthoni, P., Bernhofer, C., Davis, K., Evans, R., Fuentes, J., Goldstein, A., Katul, G., Law, B., Lee, X., Malhi, Y., Meyers, T., Munger, W., Oechel, W., Paw, K. T., Pilegaard, K., Schmid, H. P., Valentini, R., Verma, S., Vesala, T., Wilson, K., and Wofsy, S.: FLUXNET: a new tool to study the temporal and spatial variability of ecosystem–scale carbon dioxide, water vapor, and energy flux densities, B. Am. Meteorol. Soc., 82, 2415−2434, doi:10.1175/1520-0477(2001)082<2415:fantts>2.3.co;2, 2001.

Berry, J. and Bjorkman, O.: Photosynthetic response and adaptation to temperature in higher plants, Annu. Rev. Plant Phys., 31, 491−543, doi:10.1146/annurev.pp.31.060180.002423, 1980.

Bonan, G. B.: Forests and climate change: forcings, feedbacks, and the climate benefits of forests, Science, 320, 1444−1449, 2008.

Carrara, A., Kowalski, A. S., Neirynck, J., Janssens, I. A., Yuste, J. C., and Ceulemans, R.: Net ecosystem CO2 exchange of mixed forest in Belgium over 5 years, Agr. Forest Meteorol., 119, 209−227, 2003.

Carrara, A., Janssens, I. A., Curiel Yuste, J., and Ceulemans, R.: Seasonal changes in photosynthesis, respiration and NEE of a mixed temperate forest, Agr. Forest Meteorol., 126, 15−31, 2004.

Cleland, E. E., Chuine, I., Menzel, A., Mooney, H. A., and Schwartz, M. D.: Shifting plant phenology in response to global change, Trends Ecol. Evol., 22, 357−365, 2007.

Collatz, G. J., Ball, J. T., Grivet, C., and Berry, J. A.: Physiological and environmental regulation of stomatal conductance, photosynthesis and transpiration: a model that includes a laminar boundary layer, Agr. Forest Meteorol., 54, 107−136, 1991.

Collatz, G. J., Ribas-Carbo, M., and Berry, J. A.: Coupled photosynthesis-stomatal conductance model for leaves of C4 plants, Aust. J. Plant Physiol., 19, 519−538, 1992.

Cox, P. M., Betts, R. A., Jones, C. D., Spall, S. A., and Totterdell, I. J.: Acceleration of global warming due to carbon-cycle feedbacks in a coupled climate model, Nature, 408, 184−187, 2000.

Dolman, A. J., Moors, E. J., and Elbers, J. A.: The carbon uptake of a mid latitude pine forest growing on sandy soil, Agr. Forest Meteorol., 111, 157−170, 2002.

Duursma, R. A., Kolari, P., Perämäki, M., Pulkkinen, M., Mäkelä, A., Nikinmaa, E., Hari, P., Aurela, M., Berbigier, P., Bernhofer, C., Grünwald, T., Loustau, D., Mölder, M., Verbeeck, H., and Vesala, T.: Contributions of climate, leaf area index and leaf physiology to variation in gross primary production of six coniferous forests across Europe: a model-based analysis, Tree Physiol., 29, 621−639, doi:10.1093/treephys/tpp010, 2009.

Elbers, J. A., Moors, E. J., and Jacobs, C. M. J.: Gemeten Actuele Verdamping Voor Twaalf Locaties in Nederland, Rapport/STOWA, nr. 2010-36, STOWA, Amersfoort, 2010.

Elbers, J. A., Jacobs, C. M. J., Kruijt, B., Jans, W. W. P., and Moors, E. J.: Assessing the uncertainty of estimated annual totals of net ecosystem productivity: a practical approach applied to a mid latitude temperate pine forest, Agr. Forest Meteorol., 151, 1823−1830, 2011.

Epron, D., Nouvellon, Y., and Ryan, M. G.: Introduction to the invited issue on carbon allocation of trees and forests, Tree Physiol., 32, 639−643, doi:10.1093/treephys/tps055, 2012.

Falge, E., Baldocchi, D., Tenhunen, J., Aubinet, M., Bakwin, P., Berbigier, P., Bernhofer, C., Burba, G., Clement, R., Davis, K. J., Elbers, J. A., Goldstein, A. H., Grelle, A., Granier, A., Guðmundsson, J., Hollinger, D., Kowalski, A. S., Katul, G., Law, B. E., Malhi, Y., Meyers, T., Monson, R. K., Munger, J. W., Oechel, W., Paw U, K. T., Pilegaard, K., Rannik, Ü., Rebmann, C., Suyker, A., Valentini, R., Wilson, K., and Wofsy, S.: Seasonality of ecosystem respiration and gross primary production as derived from FLUXNET measurements, Agr. Forest Meteorol., 113, 53−74, 2002.

Fatichi, S. and Ivanov, V. Y.: Interannual variability of evapotranspiration and vegetation productivity, Water Resour. Res., 50, 3275−3294, 2014.

Franklin, O., Johansson, J., Dewar, R. C., Dieckmann, U., McMurtrie, R. E., Brännström, Å., and Dybzinski, R.: Modeling carbon allocation in trees: a search for principles, Tree Physiol., 32, 648−666, doi:10.1093/treephys/tpr138, 2012.

Gea-Izquierdo, G., Mäkelä, A., Margolis, H., Bergeron, Y., Black, T. A., Dunn, A., Hadley, J., Paw U, K. T., Falk, M., Wharton, S., Monson, R., Hollinger, D. Y., Laurila, T., Aurela, M., McCaughey, H., Bourque, C., Vesala, T., and Berninger, F.: Modeling acclimation of photosynthesis to temperature in evergreen conifer forests, New Phytol., 188, 175−186, doi:10.1111/j.1469-8137.2010.03367.x, 2010.

Gerten, D., Schaphoff, S., Haberlandt, U., Lucht, W., and Sitch, S.: Terrestrial vegetation and water balance-hydrological evaluation of a dynamic global vegetation model, J. Hydrol., 286, 249−270, 2004.

Goulden, M. L., Munger, J. W., Fan, S.-M., Daube, B. C., and Wofsy, S. C.: Exchange of carbon dioxide by a deciduous forest: response to interannual climate variability, Science, 271, 1576−1578, doi:10.1126/science.271.5255.1576, 1996.

Granier, A., Reichstein, M., Bréda, N., Janssens, I. A., Falge, E., Ciais, P., Grünwald, T., Aubinet, M., Berbigier, P., Bernhofer, C., Buchmann, N., Facini, O., Grassi, G., Heinesch, B., Ilvesniemi, H., Keronen, P., Knohl, A., Köstner, B., Lagergren, F., Lindroth, A., Longdoz, B., Loustau, D., Mateus, J., Montagnani, L., Nys, C., Moors, E., Papale, D., Peiffer, M., Pilegaard, K., Pita, G., Pumpanen, J., Rambal, S., Rebmann, C., Rodrigues, A., Seufert, G., Tenhunen, J., Vesala, T., and Wang, Q.: Evidence for soil water control on carbon and water dynamics in European forests during the extremely dry year: 2003, Agr. Forest Meteorol., 143, 123−145, 2007.

Haxeltine, A. and Prentice, I. C.: A general model for the light-use efficiency of primary production, Funct. Ecol., 10, 551−561, 1996a.

Haxeltine, A. and Prentice, I. C.: BIOME3: an equilibrium terrestrial biosphere model based on ecophysiological constraints, resource availability, and competition among plant functional types, Global Biogeochem. Cy., 10, 693−709, doi:10.1029/96gb02344, 1996b.

Hickler, T., Eklundh, L., Seaquist, J. W., Smith, B., Ardö, J., Olsson, L., Sykes, M. T., and Sjöström, M.: Precipitation controls Sahel greening trend, Geophys. Res. Lett., 32, L21415, doi:10.1029/2005gl024370, 2005.

Hickler, T., Prentice, I. C., Smith, B., Sykes, M. T., and Zaehle, S.: Implementing plant hydraulic architecture within the LPJ Dynamic Global Vegetation Model, Global Ecol. Biogeogr., 15, 567−577, 2006.

Hickler, T., Vohland, K., Feehan, J., Miller, P. A., Smith, B., Costa, L., Giesecke, T., Fronzek, S., Carter, T. R., Cramer, W., Kühn, I., and Sykes, M. T.: Projecting the future distribution of European potential natural vegetation zones with a generalized, tree species-based dynamic vegetation model, Global Ecol. Biogeogr., 21, 50−63, doi:10.1111/j.1466-8238.2010.00613.x, 2012.

Higgins, S. I. and Scheiter, S.: Atmospheric CO2 forces abrupt vegetation shifts locally, but not globally, Nature, 488, 209−212, 2012.

Hui, D., Luo, Y., and Katul, G.: Partitioning interannual variability in net ecosystem exchange between climatic variability and functional change, Tree Physiol., 23, 433−442, doi:10.1093/treephys/23.7.433, 2003.

Huntingford, C. and Monteith, J. L.: The behaviour of a mixed-layer model of the convective boundary layer coupled to a big leaf model of surface energy partitioning, Bound.-Layer Meteorol., 88, 87−101, doi:10.1023/a:1001110819090, 1998.

Jackson, R. B., Canadell, J., Ehleringer, J. R., Mooney, H. A., Sala, O. E., and Schulze, E. D.: A global analysis of root distributions for terrestrial biomes, Oecologia, 108, 389−411, doi:10.1007/bf00333714, 1996.

Jacobs, C. M. J., Jacobs, A. F. G., Bosveld, F. C., Hendriks, D. M. D., Hensen, A., Kroon, P. S., Moors, E. J., Nol, L., Schrier-Uijl, A., and Veenendaal, E. M.: Variability of annual CO2 exchange from Dutch grasslands, Biogeosciences, 4, 803−816, doi:10.5194/bg-4-803-2007, 2007.

Jacobs, C. M. J., Moors, E. J., Elbers, J. A., Jans, W. W. P., and Kruijt, B.: Does Inter-Annual Variability of Net Ecosystem Exchange Exceed Uncertainty?, EGU General Assembly 2009, Vienna, 2009.

James, J. C., Grace, J., and Hoad, S. P.: Growth and photosynthesis of Pinus sylvestris at its altitudinal limit in Scotland, J. Ecol., 82, 297−306, 1994.

Jarvis, N. J.: Simple physics-based models of compensatory plant water uptake: concepts and eco-hydrological consequences, Hydrol. Earth Syst. Sci., 15, 3431−3446, doi:10.5194/hess-15-3431-2011, 2011.

Keenan, T. F., Baker, I., Barr, A., Ciais, P., Davis, K., Dietze, M., Dragoni, D., Gough, C. M., Grant, R., Hollinger, D., Hufkens, K., Poulter, B., McCaughey, H., Raczka, B., Ryu, Y., Schaefer, K., Tian, H., Verbeeck, H., Zhao, M., and Richardson, A. D.: Terrestrial biosphere model performance for inter-annual variability of land-atmosphere CO2 exchange, Glob. Change Biol., 18, 1971−1987, doi:10.1111/j.1365-2486.2012.02678.x, 2012.

KNMI Klimatologie: Seizoensoverzicht – Zomer 2003 (Juni, Juli, August): Zeer Warm, Zeer Zonnig en Zeer Droog, available at: http://www.knmi.nl/klimatologie/maand_en_seizoensoverzichten/seizoen/zom03.html (last access: 12 June 2014), 2003.

KNMI Klimatologie: Seizoensoverzicht – Zomer 2005 (Juni, Juli, Augustus): Normale Temperatuur en Hoeveelheid Zonneschijn Maar Nat, available at: http://www.knmi.nl/klimatologie/maand_en_seizoensoverzichten/seizoen/zom05.html (last access: 12 June 2014), 2005.

Kramer, K., Buiteveld, J., Forstreuter, M., Geburek, T., Leonardi, S., Menozzi, P., Povillon, F., Schelhaas, M. J., Teissier du Cros, E., Vendramin, G. G., and van der Werf, D. C.: Bridging the gap between ecophysiological and genetic knowledge to assess the adaptive potential of European beech, Ecol. Model., 216, 333−353, 2008.

Kramer, K. and Hänninen, H.: The annual cycle of development of trees and process-based modelling of growth to scale up from the tree to the stand, in: Phenology of Ecosystem Processes, edited by: Noormets, A., Springer, New York, 201−227, 2009.

Kruijt, B., Jacobs, C., Moors, E., Elbers, J., Randow, C. v., Saleska, S., and Baldocchi, D.: [Presentation] Interannual variability in Net Ecosystem Exchange: is it deterministic, chaotic or random?, ICDC8: 8th International Carbon Dioxide Conference, held 13−19 September 2009, in Jena (Germany), 2009.

Lagergren, F. and Lindroth, A.: Transpiration response to soil moisture in pine and spruce trees in Sweden, Agr. Forest Meteorol., 112, 67−85, doi:10.1016/S0168-1923(02)00060-6, 2002.

Larcher, W.: Physiological Plant Ecology, Springer, Berlin, 1980.

Leemans, R. and Prentice, I. C.: FORSKA, a general forest succession model, Institute of Ecological Botany, Uppsala University, Uppsala, Sweden, PhD, 70 pp., 1989.

Lenton, T. M., Held, H., Kriegler, E., Hall, J. W., Lucht, W., Rahmstorf, S., and Schellnhuber, H. J.: Tipping elements in the Earth's climate system, P. Natl. Acad. Sci. USA, 105, 1786−1793, doi:10.1073/pnas.0705414105, 2008.

Linder, S. and Troeng, E.: Photosynthesis and transpiration of 20-year-old scots pine, in: Structure and function of northern coniferous forests–an ecosystem study, edited by: Persson, T., Ecological Bulletins, 32, 165−181, 1980.

Litton, C. M., Raich, J. W., and Ryan, M. G.: Carbon allocation in forest ecosystems, Glob. Change Biol., 13, 2089−2109, doi:10.1111/j.1365-2486.2007.01420.x, 2007.

Luyssaert, S., Janssens, I. A., Sulkava, M., Papale, D., Dolman, A. J., Reichstein, M., Hollmén, J., Martin, J. G., Suni, T., Vesala, T., Loustau, D., Law, B. E., and Moors, E. J.: Photosynthesis drives anomalies in net carbon-exchange of pine forests at different latitudes, Glob. Change Biol., 13, 2110−2127, doi:10.1111/j.1365-2486.2007.01432.x, 2007.

McDowell, N., Pockman, W. T., Allen, C. D., Breshears, D. D., Cobb, N., Kolb, T., Plaut, J., Sperry, J., West, A., Williams, D. G., and Yepez, E. A.: Mechanisms of plant survival and mortality during drought: why do some plants survive while others succumb to drought?, New Phytol., 178, 719−739, doi:10.1111/j.1469-8137.2008.02436.x, 2008.

Medlyn, B. E., Zaehle, S., De Kauwe, M. G., Walker, A. P., Dietze, M. C., Hanson, P. J., Hickler, T., Jain, A. K., Luo, Y., Parton, W., Prentice, I. C., Thornton, P. E., Wang, S., Wang, Y.-P., Weng, E., Iversen, C. M., McCarthy, H. R., Warren, J. M., Oren, R., and Norby, R. J.:

Using ecosystem experiments to improve vegetation models, Nature Climate Change, 5, 528−534, 2015.

Moors, E. J.: Water Use of Forests in the Netherlands, Vrije Universiteit Amsterdam, the Netherlands, Vrije Universiteit Amsterdam, Amsterdam The Netherlands, 290 pp., 2012.

Moors, E. J., Elbers, J. A., Hutjes, R. W. A., Jacobs, C., Jans, W. W. P., Kruijt, B., Stolk, P., ter Maat, H., Vermeulen, M., Abreu, P., and Dolman, A. J.: Inter-annual variability of carbon exchange and extreme events at the Loobos pine forest, in preparation, 2014.

Morales, P., Sykes, M. T., Prentice, I. C., Smith, P., Smith, B., Bugmann, H., Zierl, B., Friedlingstein, P., Viovy, N., Sabaté, S., Sánchez, A., Pla, E., Gracia, C. A., Sitch, S., Arneth, A., and Ogee, J.: Comparing and evaluating process-based ecosystem model predictions of carbon and water fluxes in major European forest biomes, Glob. Change Biol., 11, 2211−2233, doi:10.1111/j.1365-2486.2005.01036.x, 2005.

Naeem, S.: Ecosystem consequences of biodiversity loss: the evolution of a paradigm, Ecology, 83, 1537−1552, doi:10.1890/0012-9658(2002)083[1537:ecoblt]2.0.co;2, 2002.

Peylin, P., Bousquet, P., Le Quéré, C., Sitch, S., Friedlingstein, P., McKinley, G., Gruber, N., Rayner, P., and Ciais, P.: Multiple constraints on regional CO2 flux variations over land and oceans, Global Biogeochem. Cy., 19, GB1011, doi:10.1029/2003gb002214, 2005.

Pitman, A. J., de Noblet-Ducoudré, N., Cruz, F. T., Davin, E. L., Bonan, G. B., Brovkin, V., Claussen, M., Delire, C., Ganzeveld, L., Gayler, V., van den Hurk, B. J. J. M., Lawrence, P. J., van der Molen, M. K., Müller, C., Reick, C. H., Seneviratne, S. I., Strengers, B. J., and Voldoire, A.: Uncertainties in climate responses to past land cover change: first results from the LUCID intercomparison study, Geophys. Res. Lett., 36, L14814, doi:10.1029/2009gl039076, 2009.

Rammig, A., Jupp, T., Thonicke, K., Tietjen, B., Heinke, J., Ostberg, S., Lucht, W., Cramer, W., and Cox, P.: Estimating the risk of Amazonian forest dieback, New Phytol., 187, 694−706, doi:10.1111/j.1469-8137.2010.03318.x, 2010.

Reichstein, M., Falge, E., Baldocchi, D., Papale, D., Aubinet, M., Berbigier, P., Bernhofer, C., Buchmann, N., Gilmanov, T., Granier, A., Grünwald, T., Havránková, K., Ilvesniemi, H., Janous, D., Knohl, A., Laurila, T., Lohila, A., Loustau, D., Matteucci, G., Meyers, T., Miglietta, F., Ourcival, J.-M., Pumpanen, J., Rambal, S., Rotenberg, E., Sanz, M., Tenhunen, J., Seufert, G., Vaccari, F., Vesala, T., Yakir, D., and Valentini, R.: On the separation of net ecosystem exchange into assimilation and ecosystem respiration: review and improved algorithm, Glob. Change Biol., 11, 1424−1439, doi:10.1111/j.1365-2486.2005.001002.x, 2005.

Sandström, F., Petersson, H., Kruys, N., and Ståhl, G.: Biomass conversion factors (density and carbon concentration) by decay classes for dead wood of Pinus sylvestris, Picea abies and Betula spp. in boreal forests of Sweden, Forest Ecol. Manag., 243, 19−27, doi:10.1016/j.foreco.2007.01.081, 2007.

Schelhaas, M. J., Nabuurs, G. J., Jans, W. W. P., Moors, E. J., Sabaté, S., and Daamen, W. P.: Closing the carbon budget of a Scots pine forest in the Netherlands, Climatic Change, 67, 309−328, 2004.

Schurgers, G., Hickler, T., Miller, P. A., and Arneth, A.: European emissions of isoprene and monoterpenes from the Last Glacial Maximum to present, Biogeosciences, 6, 2779−2797, doi:10.5194/bg-6-2779-2009, 2009.

Sevanto, S., Suni, T., Pumpanen, J., Grönholm, T., Kolari, P., Nikinmaa, E., Hari, P., and Vesala, T.: Wintertime photosynthesis and water uptake in a boreal forest, Tree Physiol., 26, 749−757, doi:10.1093/treephys/26.6.749, 2006.

Sierra, C. A., Loescher, H. W., Harmon, M. E., Richardson, A. D., Hollinger, D. Y., and Perakis, S. S.: Interannual variation of carbon fluxes from three contrasting evergreen forests: the role of forest dynamics and climate, Ecology, 90, 2711−2723, doi:10.1890/08-0073.1, 2009.

Sitch, S., Smith, B., Prentice, I. C., Arneth, A., Bondeau, A., Cramer, W., Kaplan, J. O., Levis, S., Lucht, W., Sykes, M. T., Thonicke, K., and Venevsky, S.: Evaluation of ecosystem dynamics, plant geography and terrestrial carbon cycling in the LPJ dynamic global vegetation model, Glob. Change Biol., 9, 161−185, 2003.

Sitch, S., Huntingford, C., Gedney, N., Levy, P. E., Lomas, M., Piao, S. L., Betts, R., Ciais, P., Cox, P., Friedlingstein, P., Jones, C. D., Prentice, I. C., and Woodward, F. I.: Evaluation of the terrestrial carbon cycle, future plant geography and climate-carbon cycle feedbacks using five Dynamic Global Vegetation Models (DGVMs), Glob. Change Biol., 14, 2015−2039, doi:10.1111/j.1365-2486.2008.01626.x, 2008.

Sitch, S., Friedlingstein, P., Gruber, N., Jones, S. D., Murray-Tortarolo, G., Ahlström, A., Doney, S. C., Graven, H., Heinze, C., Huntingford, C., Levis, S., Levy, P. E., Lomas, M., Poulter, B., Viovy, N., Zaehle, S., Zeng, N., Arneth, A., Bonan, G., Bopp, L., Canadell, J. G., Chevallier, F., Ciais, P., Ellis, R., Gloor, M., Peylin, P., Piao, S., Le Quéré, C., Smith, B., Zhu, Z., and Myneni, R.: Trends and drivers of regional sources and sinks of carbon dioxide over the past two decades, Biogeosciences Discuss., 10, 20113−20177, doi:10.5194/bgd-10-20113-2013, 2013.

Smith, B., Prentice, I. C., and Sykes, M. T.: Representation of vegetation dynamics in the modelling of terrestrial ecosystems: comparing two contrasting approaches within European climate space, Global Ecol. Biogeogr., 10, 621−637, doi:10.1046/j.1466-822X.2001.t01-1-00256.x, 2001.

Smith, N. G. and Dukes, J. S.: Plant respiration and photosynthesis in global-scale models: incorporating acclimation to temperature and CO2, Glob. Change Biol., 19, 45−63, doi:10.1111/j.1365-2486.2012.02797.x, 2013.

Suni, T., Berninger, F., Markkanen, T., Keronen, P., Rannik, Ü., and Vesala, T.: Interannual variability and timing of growing-season CO2 exchange in a boreal forest, J. Geophys. Res., 108, 4265, doi:10.1029/2002jd002381, 2003a.

Suni, T., Berninger, F., Vesala, T., Markkanen, T., Hari, P., Mäkelä, A., Ilvesniemi, H., Hänninen, H., Nikinmaa, E., Huttula, T., Laurila, T., Aurela, M., Grelle, A., Lindroth, A., Arneth, A., Shibistova, O., and Lloyd, J.: Air temperature triggers the recovery of evergreen boreal forest photosynthesis in spring, Glob. Change Biol., 9, 1410−1426, doi:10.1046/j.1365-2486.2003.00597.x, 2003b.

Teskey, R. O., Whitehead, D., and Linder, S.: Photosynthesis and carbon gain by pines, Ecol. Bull., in: Environmental constraints on the structure and productivity of pine forest ecosystems: a comparative analysis, edited by: Gholz, H. L., Linder, S., and McMurtrie, R. E., Ecological Bulletins, 43, 35−49, 1994.

Teuling, A. J., Seneviratne, S. I., Stockli, R., Reichstein, M., Moors, E., Ciais, P., Luyssaert, S., van den Hurk, B., Ammann, C., Bernhofer, C., Dellwik, E., Gianelle, D., Gielen, B., Grunwald, T., Klumpp, K., Montagnani, L., Moureaux, C., Sottocornola, M., and Wohlfahrt, G.: Contrasting response of European forest and grassland energy exchange to heatwaves, Nat. Geosci., 3, 722−727, 2010.

Thomas, S. C. and Martin, A. R.: Carbon content of tree tissues: a synthesis, Forests, 3, 332−352, 2012.

van den Hurk, B. J. J. M., Viterbo, P., and Los, S. O.: Impact of leaf area index seasonality on the annual land surface evaporation in a global circulation model, J. Geophys. Res., 108, 4191, doi:10.1029/2002jd002846, 2003.

van der Werf, G. W., Sass-Klaassen, U. G. W., and Mohren, G. M. J.: The impact of the 2003 summer drought on the intra-annual growth pattern of beech (Fagus sylvatica L.) and oak (Quercus robur L.) on a dry site in the Netherlands, Dendrochronologia, 25, 103−112, 2007.

Verbeeck, H., Peylin, P., Bacour, C., Bonal, D., Steppe, K., and Ciais, P.: Seasonal patterns of CO2 fluxes in Amazon forests: fusion of eddy covariance data and the ORCHIDEE model, J. Geophys. Res.-Biogeo., 116, G02018, doi:10.1029/2010jg001544, 2011.

Weber, U., Jung, M., Reichstein, M., Beer, C., Braakhekke, M. C., Lehsten, V., Ghent, D., Kaduk, J., Viovy, N., Ciais, P., Gobron, N., and Rödenbeck, C.: The interannual variability of Africa's ecosystem productivity: a multi-model analysis, Biogeosciences, 6, 285−295, doi:10.5194/bg-6-285-2009, 2009.

Williams, C. A., Hanan, N. P., Baker, I., Collatz, G. J., Berry, J., and Denning, A. S.: Interannual variability of photosynthesis across Africa and its attribution, J. Geophys. Res., 113, G04015, doi:10.1029/2008jg000718, 2008.

Wolkovich, E. M., Cook, B. I., Allen, J. M., Crimmins, T. M., Betancourt, J. L., Travers, S. E., Pau, S., Regetz, J., Davies, T. J., Kraft, N. J. B., Ault, T. R., Bolmgren, K., Mazer, S. J., McCabe, G. J., McGill, B. J., Parmesan, C., Salamin, N., Schwartz, M. D., and Cleland, E. E.: Warming experiments underpredict plant phenological responses to climate change, Nature, 485, 494−497, doi:10.1038/nature11014, 2012.

Wramneby, A., Smith, B., Zaehle, S., and Sykes, M. T.: Parameter uncertainties in the modelling of vegetation dynamics-Effects on tree community structure and ecosystem functioning in European forest biomes, Ecol. Model., 216, 277−290, 2008.

Wramneby, A., Smith, B., and Samuelsson, P.: Hot spots of vegetation-climate feedbacks under future greenhouse forcing in Europe, J. Geophys. Res.-Atmos., 115, D21119, doi:10.1029/2010jd014307, 2010.

Yamamoto, S., Murayama, S., And, N. S., and Kondo, H.: Seasonal and inter-annual variation of CO2 flux between a temperate forest and the atmosphere in Japan, Tellus B, 51, 402−413, doi:10.1034/j.1600-0889.1999.00020.x, 1999.

Yuan, W., Luo, Y., Richardson, A. D., Oren, R., Luyssaert, S., Janssens, I. A., Ceulemans, R., Zhou, X., Grünwald, T., Aubinet, M., Berhofer, C., Baldocchi, D. D., Chen, J., Dunn, A. L., Deforest, J. L., Dragoni, D., Goldstein, A. H., Moors, E., Munger, J. W., Monson, R. K., Suyker, A. E., Starr, G., Scott, R. L., Tenhunen, J., Verma, S. B., Vesala, T., and Wofsy, S. T. E.: Latitudinal patterns of magnitude and interannual variability in net ecosystem exchange regulated by biological and environmental variables, Glob. Change Biol., 15, 2905−2920, doi:10.1111/j.1365-2486.2009.01870.x, 2009.

Zaehle, S., Sitch, S., Smith, B., and Hatterman, F.: Effects of parameter uncertainties on the modeling of terrestrial biosphere dynamics, Global Biogeochem. Cy., 19, GB3020, doi:10.1029/2004gb002395, 2005.

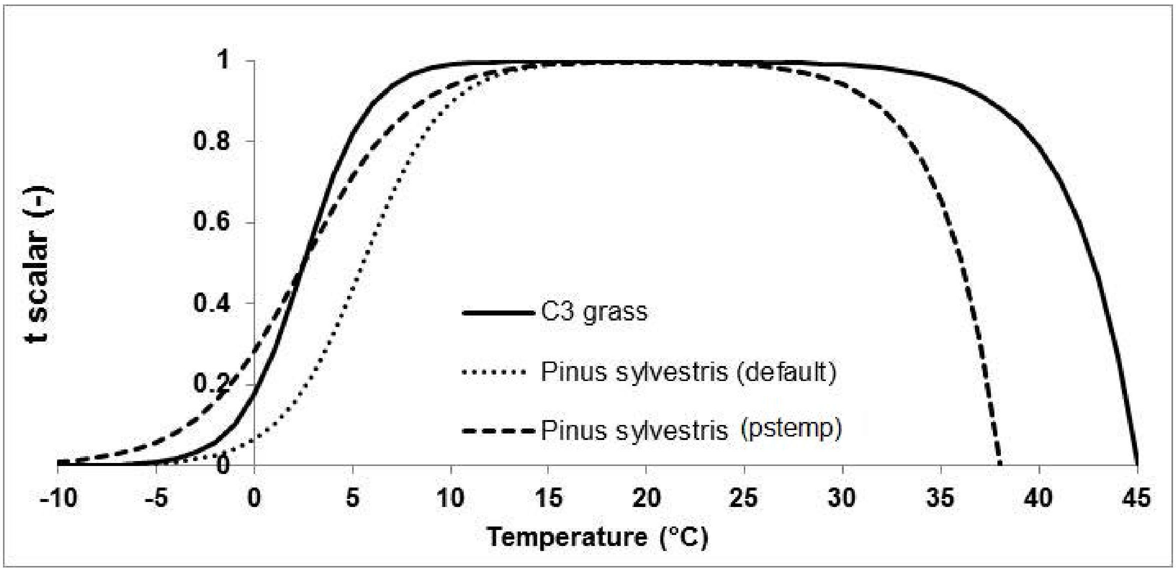

Figure 1. Temperature function (t_{scalar}) for *Pinus sylvestris* and C_3 grass, values between 0 (photosynthesis maximally limited by temperature scalar) and 1 (photosynthesis not limited by temperature scalar). Default settings for *P*. *sylvestris* (dotted line: $pstemp_{min}$ = −4 °C, optimum 15–25 °C, $pstemp_{max}$ = 37 °C) and C_3 grass (solid line: $pstemp_{min}$ = −5 °C, optimum 10–35 °C, $pstemp_{max}$ = 45 °C). Changed parameterization (*pstemp*) for *P*. *sylvestris* ($pstemp_{min}$ = −10 °C, optimum 15–25 °C, $pstemp_{max}$ = 37 °C).

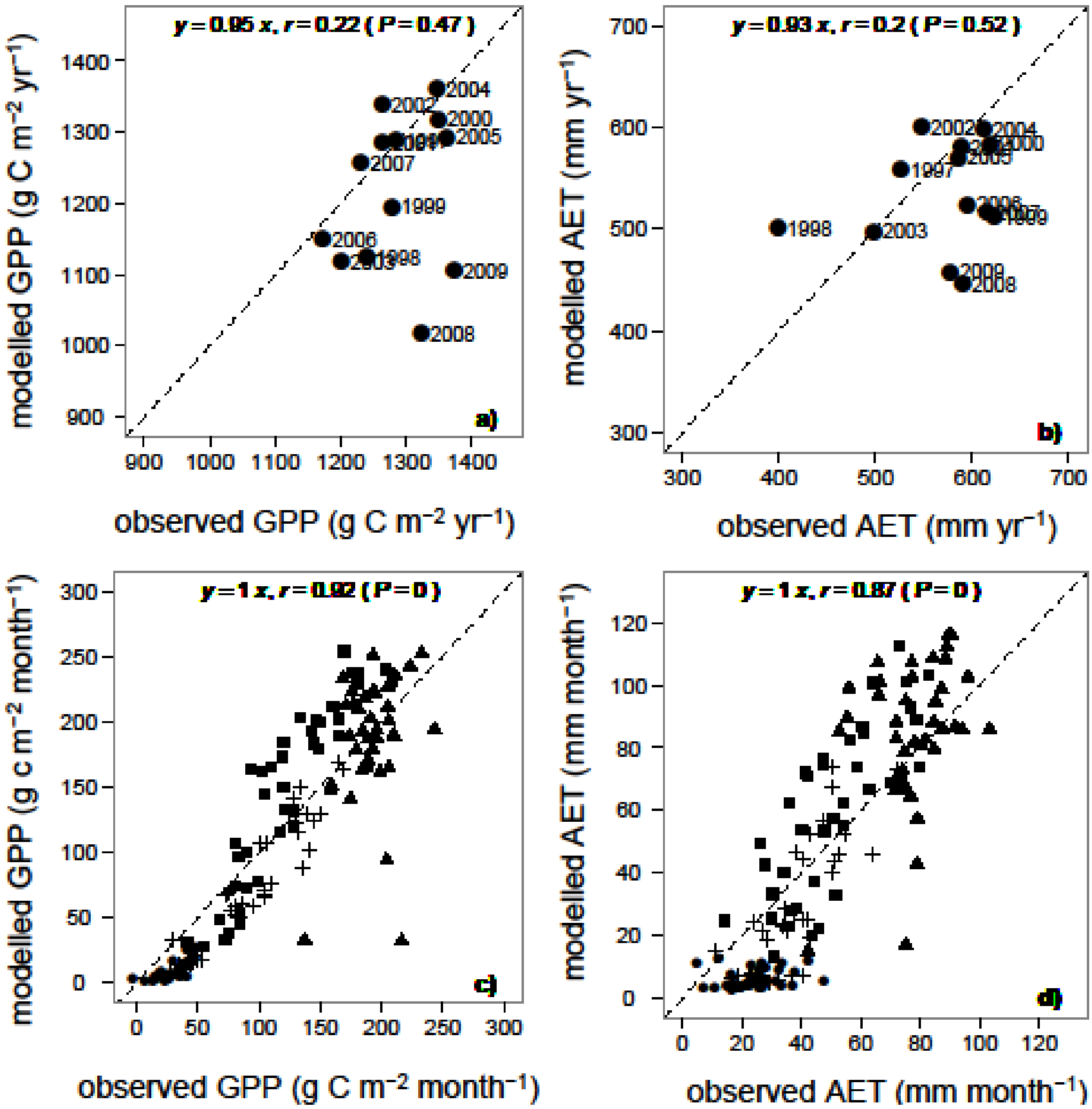

Figure 2. Observed vs. modelled variability in GPP **(a, c)** and AET **(b, d)** for the default model scenario (S1) on the annual time scale **(a, b)** and monthly time scale **(c, d)**. Dotted line is the 1 : 1 line. The equation shows linear regression through the origin, with correlation coefficients. Fluxes are hatched per season for subpanels **(c)** and **(d)**: ● = winter (December, January, February); ■ = spring (March, April, May); ▲ = summer (June, July, August); + = fall (September, October, November).

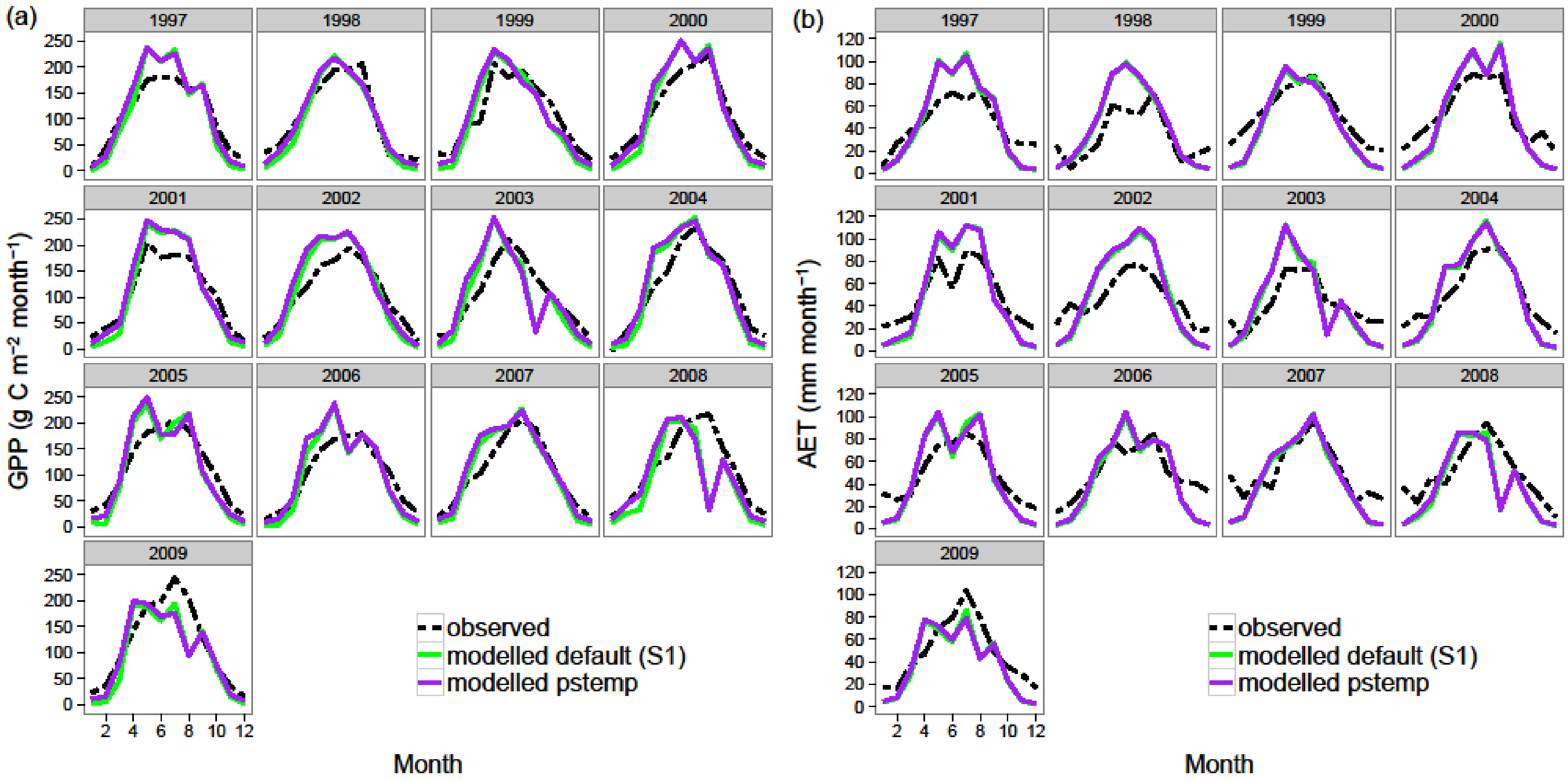

Figure 3. Observed (black dotted line) and modelled values for default (S1, green line) and changed temperature response (*pstemp*, purple line) runs. **(a)** Monthly values for GPP (g C m^{-2} month^{-1}). **(b)** Monthly values for AET (mm month^{-1}).

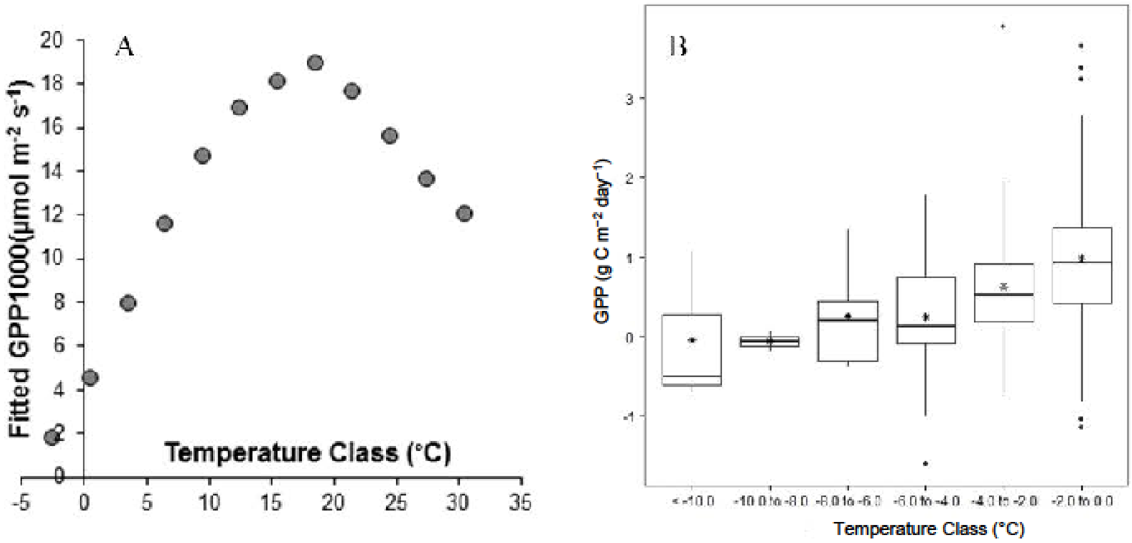

Figure 4. Observed temperature responses at Loobos. **(A)** Courtesy of P. Abreu: fitted GPP at a solar light intensity of 1000 Wm^{-2} (GPP1000, μmol m^{-2} s^{-1}) based on half-hourly EC measurements (1997–2011) following Jacobs et al. (2007); **(B)** daily GPP (g C m^{-2} day^{-1}) observed at Loobos calculated from site EC measurements, for days with average daily temperatures < 0 °C and total net radiation received > 2 MJ day^{-1} (n = 175).

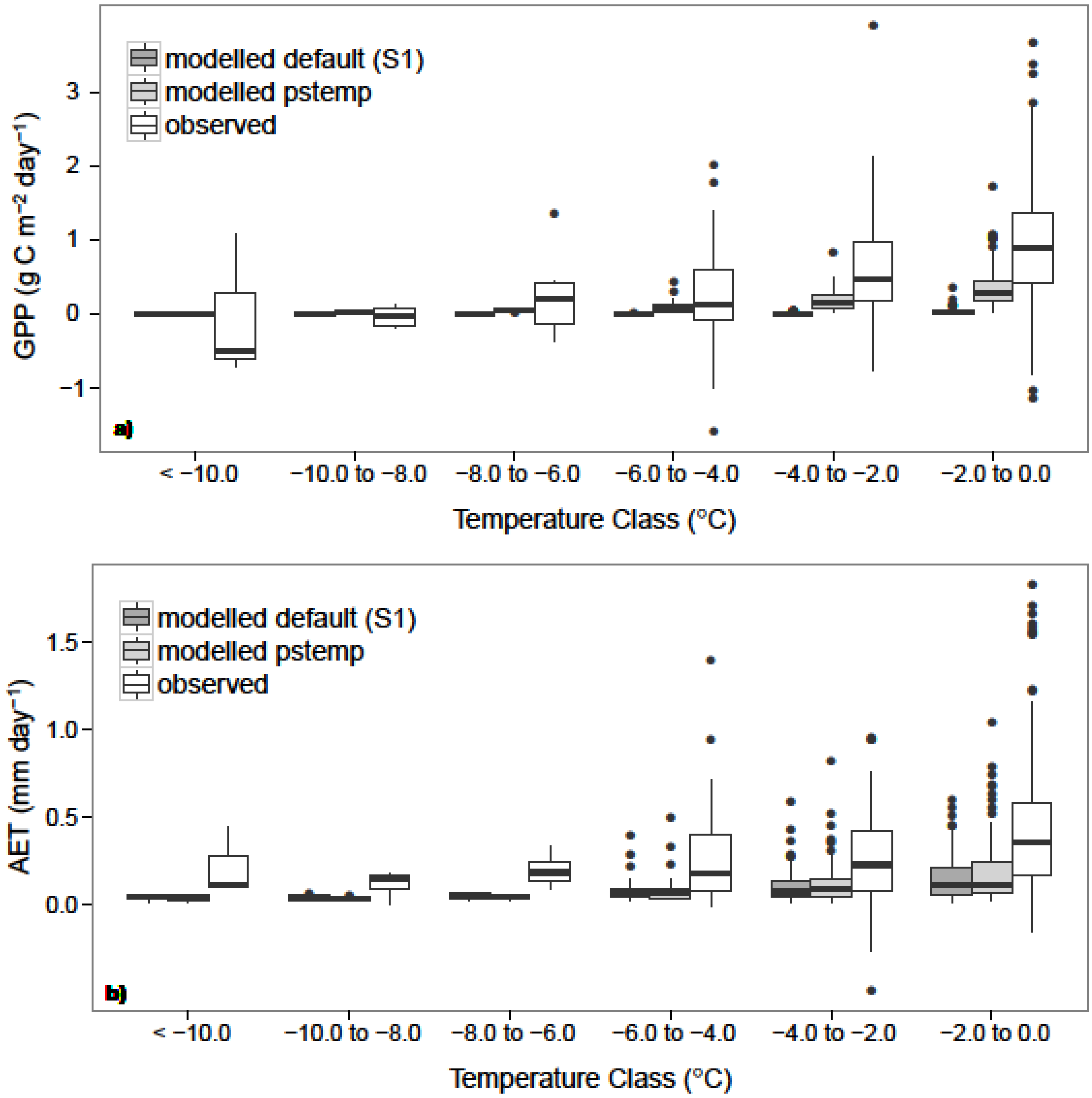

Figure 5. Effect of change in temperature scalar t_{scalar} on modelled estimates of **(a)** GPP (g C m^{-2} day^{-1}) and **(b)** AET (mm day^{-1}). $pstemp_{min}$ for *Pinus sylvestris* is set to −10 °C, other values remain unchanged. (White: observed values, dark grey: modelled default (S1), light grey: changed t_{scalar} function (*pstemp*)). Results for days with net radiation > 2 MJ day^{-1}.

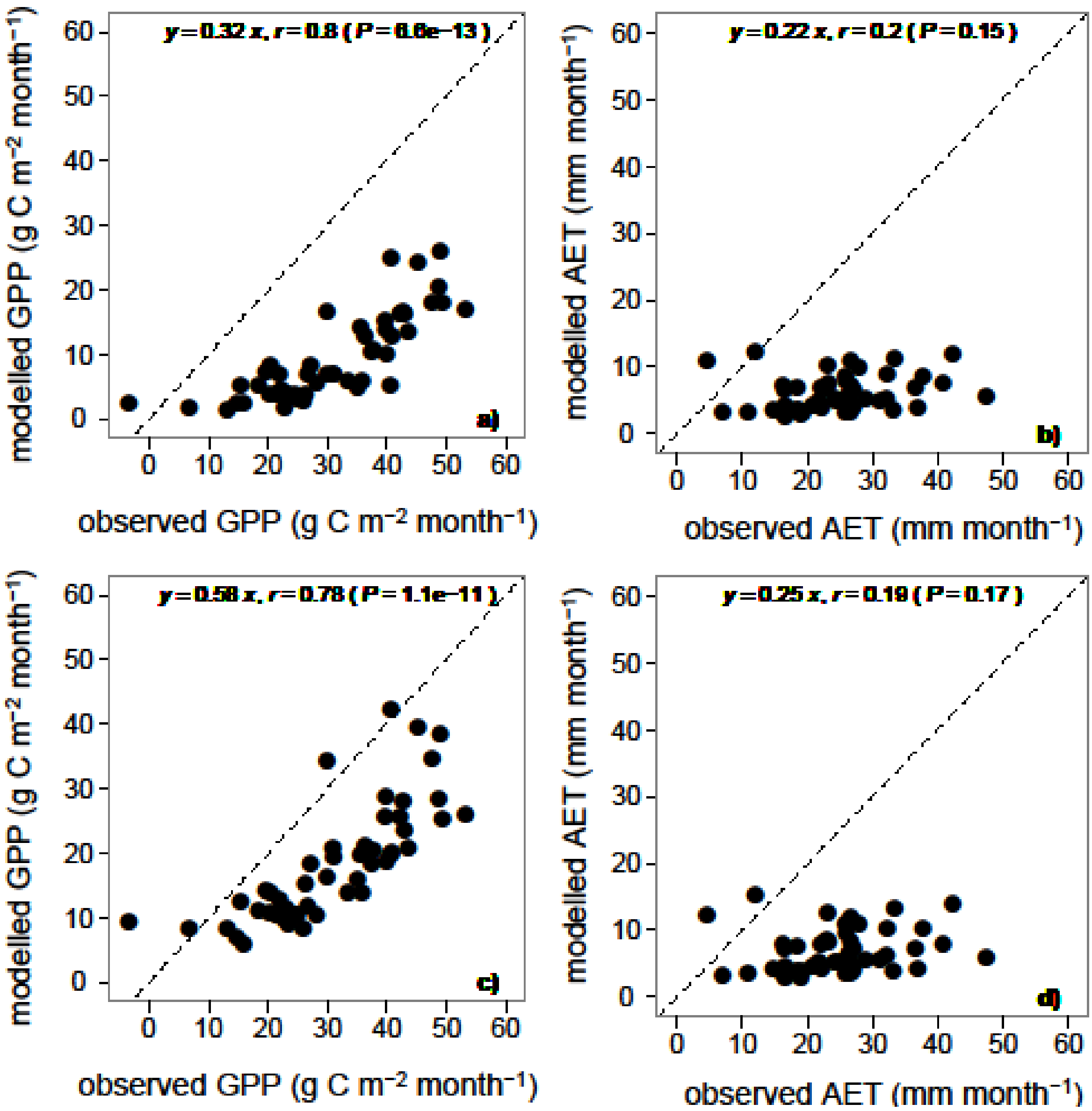

Figure 6. Variability during winter on monthly time scale for **(a, b)** GPP (g C m^{-2} month^{-1}); and **(c, d)** AET (mm month^{-1}), between default settings (S1, **a** and **c**) and changed t_{scalar} (*pstemp*, **b** and **d**) during winter. All days in December, January and February are included (i.e., no selection for radiation). All slopes significantly differed from 1.0 ($P < 0.05$). RMSE values: **(a)** 22.7, **(b)** 20.4, **(c)** 14.7, **(d)** 19.7.

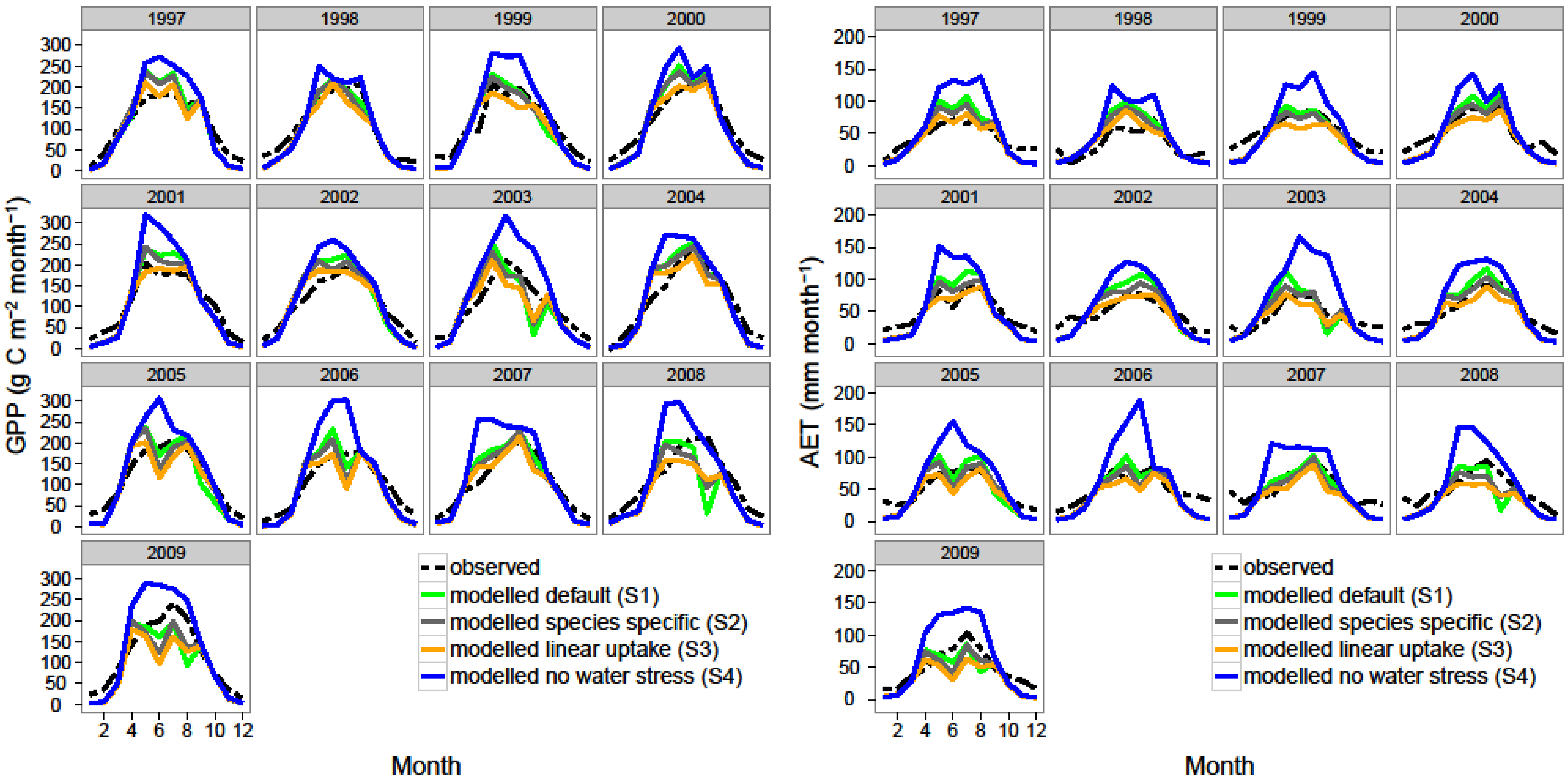

Figure 7. Comparison of fluxes for **(a)** GPP (g C m^{-2} month^{-1}) and **(b)** AET (mm month^{-1}) using different water uptake functions. Dotted line: observed values. Solid lines: modelled values for scenarios S1–S4.

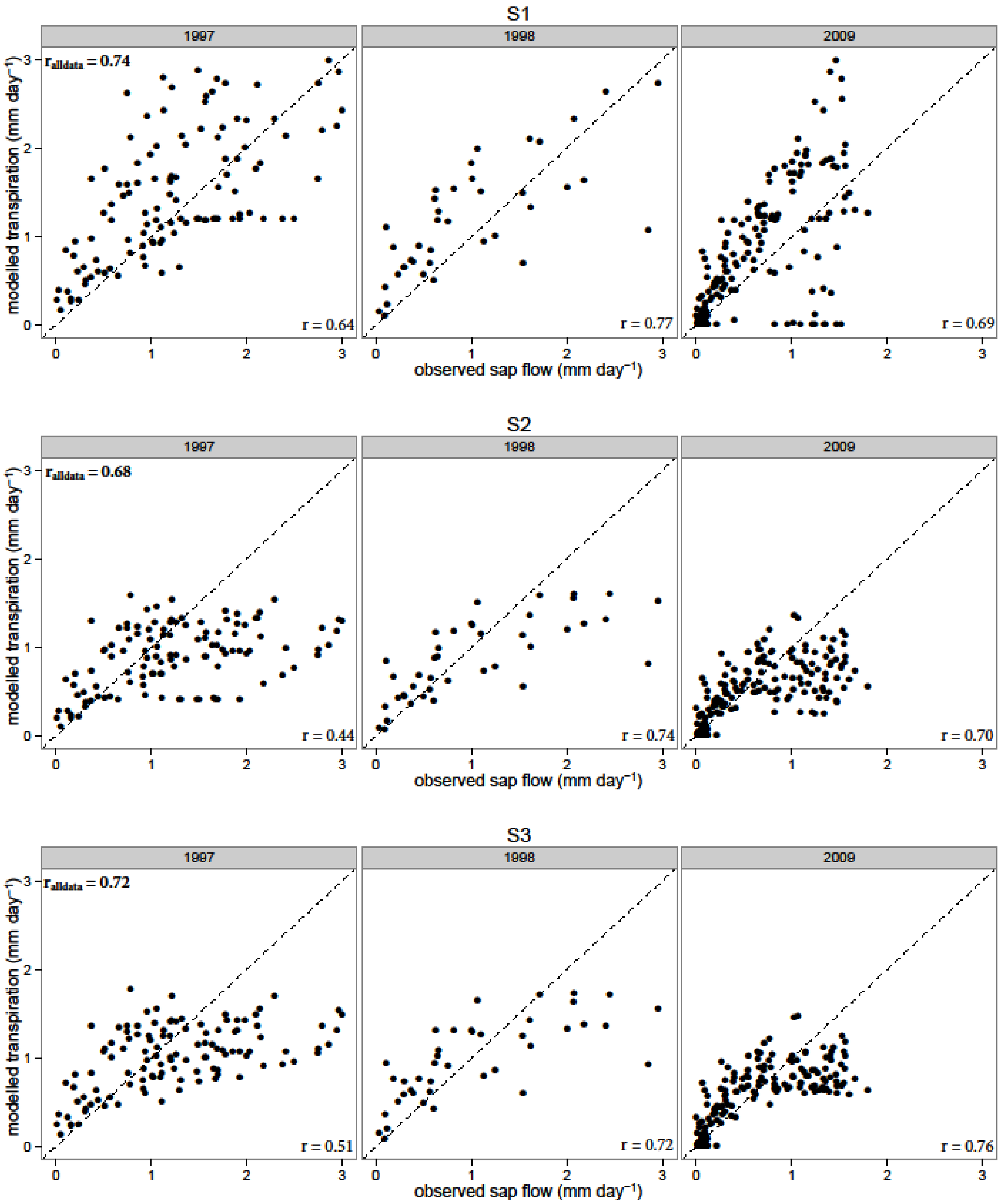

Figure 8. Modelled transpiration (mm day^{-1}) for *Pinus sylvestris*, compared to observed sap flow (mm day^{-1}). Pearson correlation coefficients significantly different from 0 ($P < 0.01$) for all separate years as well as all data points together ($r_{alldata}$). Sap flow measurements for 1997 and 1998 acquired using tissue heat balance systems; and for 2009 using Granier thermal dissipation probes. S1 = default uptake, S2 = species specific uptake, S3 = linear uptake.

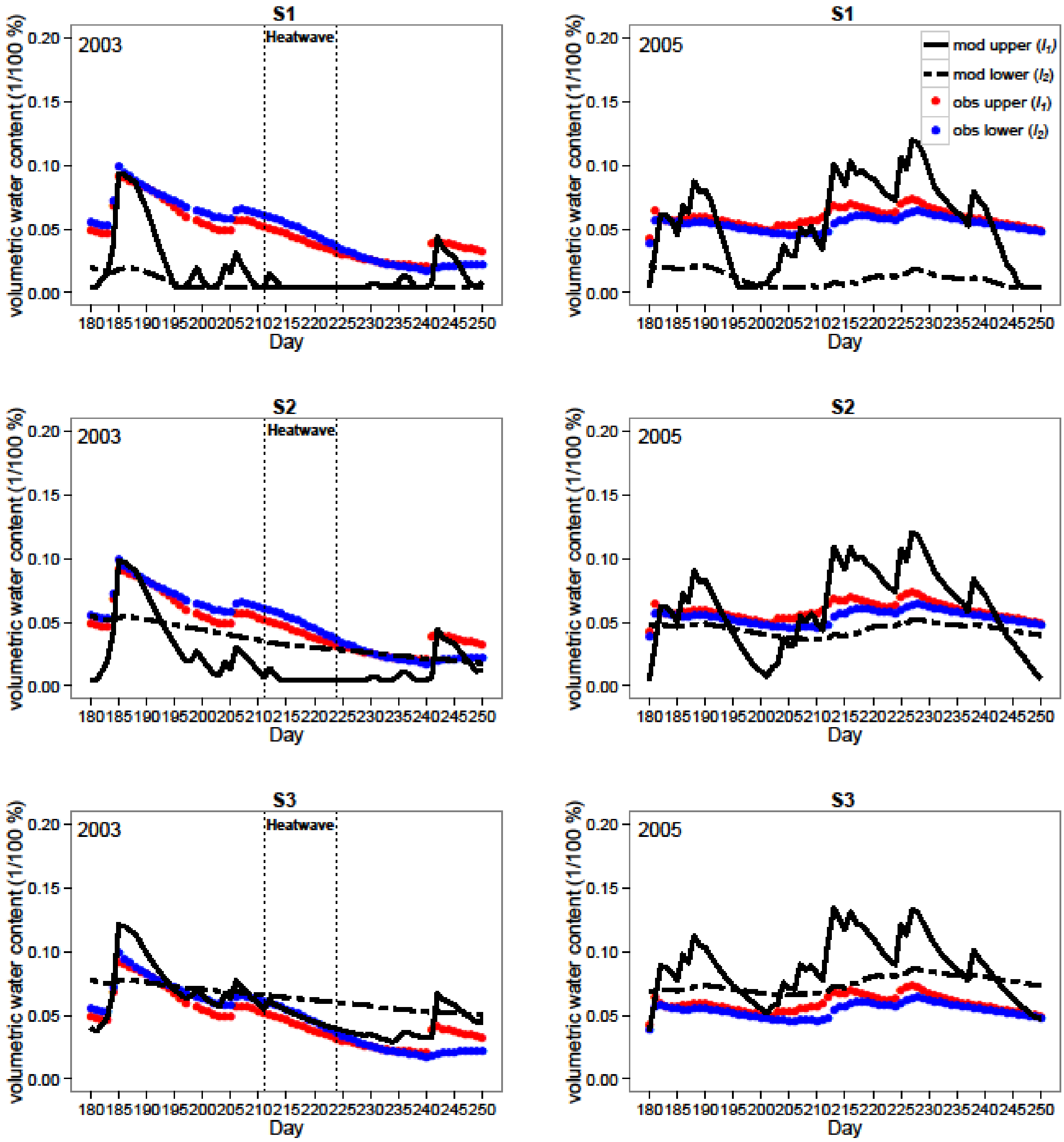

Figure 9. Daily modelled (mod, black lines) and observed (obs, red and blue) soil moisture (as volumetric water content, 1/100%) for summer of 2003 and 2005. The two depths refer to the two soil layers in LPJ-GUESS: l_1 (0–50 cm) and l_2 (50–150 cm). For 2003, the heatwave period is indicated between the black lines.

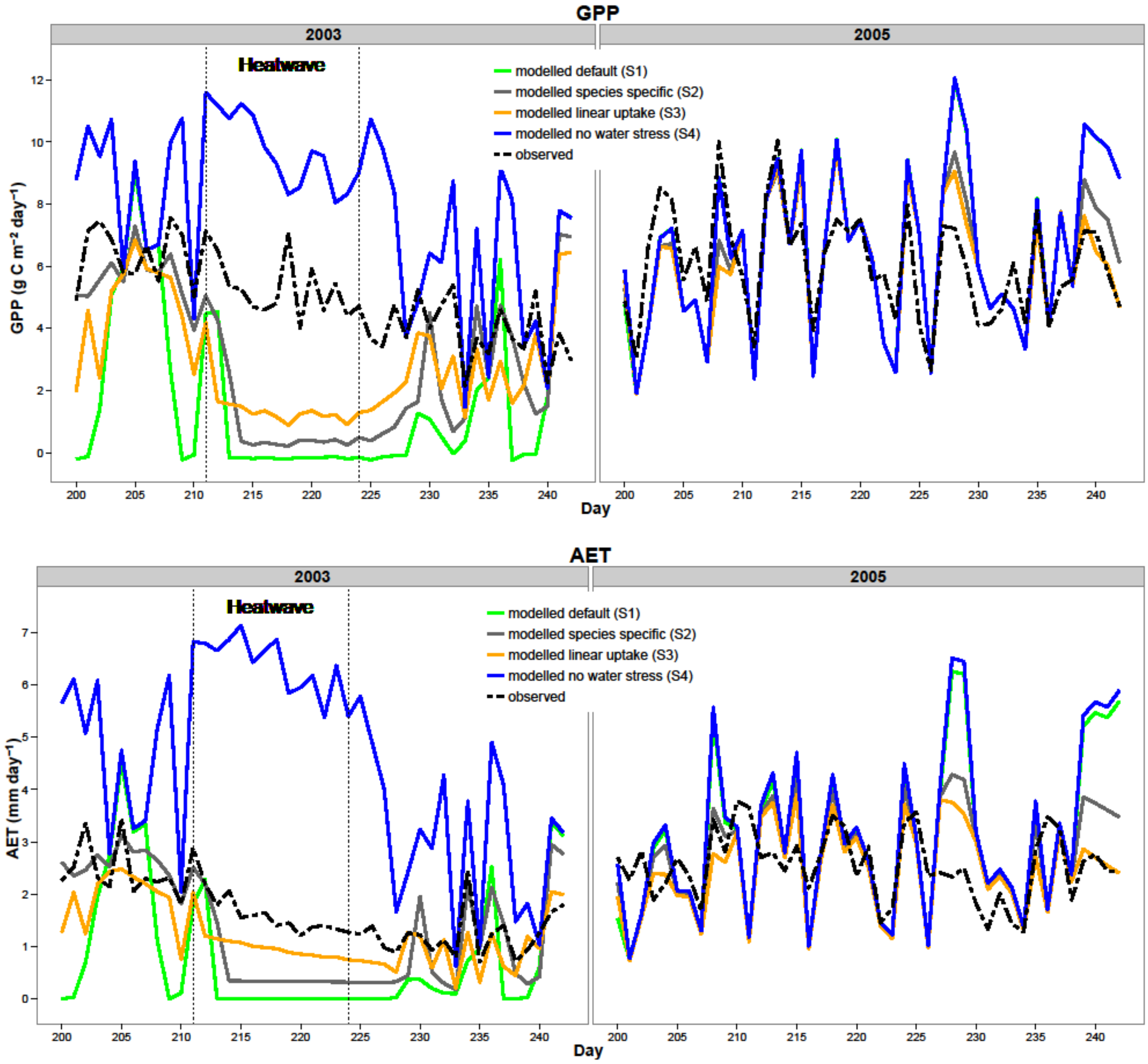

Figure 10. Daily observed and modelled fluxes for **(a)** GPP (g C day^{-1}) and **(b)** AET (mm day^{-1}) for July and August in two different climate years. In summer 2003 a heatwave and corresponding drought occurred in Europe (e.g. see Teuling et al., 2010). Based on long term averages of the Dutch Royal Metereological Institute (KNMI), higher temperatures, more sunshine hours and much less precipitation was received during this summer, and an official heatwave took place in The Netherlands during August (KNMI, 2003). The KNMI defines a heatwave as a period of at least 5 consecutive days in which the maximum temperature exceeds 25 °C, provided that on at least 3 days in this period the maximum temperature exceeds 30 °C. Based on these criteria, heatwave duration was from 31 July to 13 August and is marked in the graph by two dotted black vertical lines. The summer of 2005 had average temperatures and sunshine but was much wetter, and August was a month with particularly high precipitation compared to long term averages (KNMI, 2005).

Table 1. Parameter values for LPJ-GUESS. Values for this study are similar to Hickler et al. (2012), Table S1.1, except for values in bold font. T_{c,max_est} = maximum coldest-month temperature for establishment; $drought_{tol}$ = drought tolerance level of a species (0 = very tolerant, 1 = not at all tolerant); $root_{distr[l1]}$ = fraction of roots in first soil layer (the remainder being allocated to second soil layer); *sla* = specific leaf area.

Species/PFT	Growth form	T_{c,max_est} (°C)	$drought_{tol}$[a] (−)	$root_{distr[l1]}$ (−)	sla (m^2/kg C)
Pinus sylvestris	tree	**limitless**	0.25	0.6	**9.3**[b]
C_3 herbaceous	herbaceous	limitless	0.01	0.9	32.4

[a] Similar to *fAWC* in Hickler et al. 2012, called drought tolerance here. Not always used by model, only when using species specific water uptake from the soil (model setup S2, *wr_speciesspecific*).
[b] Value based on site measurements by Wilma Jans et al. (1997, unpublished data, available at http://www.climatexchange.nl/sites/loobos/) and Katrin Fleischer (2013, unpublished data).

Table 2. Modelled and observed site characteristics of Loobos. All modelled values for biomass are calculated for the period 1997–2009, and multiplied by a factor 0.82 to exclude root biomass (taken from Jackson et al. (1996) as a topical value for conifer forests).

	Aboveground biomass (kg C m^{-2})	**LAI**	
		Pinus sylvestris	C_3 grass
Observed:	4.98[a]	1.62[b]	1.0[c]
Modelled:			
Default/S1	5.95 ± 0.10	1.5	2.4
pstemp	7.18 ± 0.14	1.7	1.9
S2	4.55 ± 0.11	1.1	3.6
S3	4.72 ± 0.11	1.2	2.8
S4	7.64 ± 0.19	1.8	2.6

[a] 9.23 kg m^{-2} standing biomass in 1997, annual growth increment of 0.124 kg m^{-2} (data source: http://www.climatexchange.nl/sites/loobos/). To convert to carbon mass a factor of 0.5 was used (e.g. see Sandström et al., 2007; Thomas and Martin, 2012), resulting in an estimated average aboveground biomass between 1997–2009 of 4.98 kg C m^{-2}.

[b] Measured average tree LAI from 1997–2009 (unpublished data), minimum 1.44 (2007), maximum 1.78 (2009), standard deviation is 0.10. Dolman et al. (2002) report maximum LAI of 1.9 for 1997.

[c] Measurements between 1999 and 2002 (n = 52), standard deviation 0.4 m^2 m^{-2} (unpublished data).

Table 3. Goodness-of-fit values for model scenarios S1–S4 and changed temperature response function, "*pstemp*". Correlation coefficient (*r*), and Root Mean Square Error (RMSE) for daily, monthly and annual data. Bold values represent data distributions that are identical using the Wilcoxon ranking test.

	GPP						AET					
	annual		monthly		daily		annual		monthly		daily	
Run	r	RMSE	r	RMSE	r	RMSE	r	RMSE	r	RMSE	r	RMSE
Default/S1	**0.22**	125.9	0.92*	35.7	0.79*	2.20	**0.20**	77.7	**0.87***	19.7	0.62*	1.27
pstemp	**0.16**	109.3	**0.90***	36.3	0.78*	2.15	**0.21**	73.4	**0.87***	19.6	0.62	1.25
S2	0.32	128.6	0.92*	32.6	0.81*	1.93	0.19	90.8	0.87*	17.2	0.65*	1.03
S3	0.27	198.9	0.92*	31.4	0.81*	1.78	0.13	141.9	0.86*	17.3	0.65*	0.94
S4	0.24	231.3	0.94*	51.9	0.85*	2.45	0.31	168.3	0.88*	36.2	0.68*	1.67

* Significance tests for Pearson correlation: *P* value < 0.05.